Recent Works in My Lab.

- Magnetism
  - Chiral magnetism
  - Low dimensional magnetism in TiOBr & VOCl
  - Magnetism in $(La,Ca)_2CoO_4$

- Superconductivity
  - Two gap superconductivity in Y_2C_3
  - Type-I superconductivity in B-doped SiC
  - Interlayer phonon driven superconductivity in CaAlSi

Spin, charge and orbital orders in two-dimensional $La_{2-x}Ca_xCoO_4$

Department of Physics and Mathematics, Aoyama Gakuin University

Jun Akimitsu

DC3 Kazumasa Horigane

Outline

- **Introduction**

  Summary of the previous works in $La_{2-x}Sr_xCoO_4$

  Purpose of the present study in $La_{2-x}Ca_{\boldsymbol{x}}CoO_4$

- **Results and discussion**

  Single crystal growth and structure analysis

  Resonant X-ray scattering

  Neutron diffraction measurements

  Ultrasound measurements

- **Summary**

Collaborators

Crystal growth of $La_{2-x}Sr_xCoO_4$ and their physical properties

Kazumasa Horigane, Toru Uchida (Aoyama-Gakuin Univ.)

Crystal structure analysis

Yukio Noda（Tohoku University）、Yusuke Kousaka（Aoyama-Gakuin Univ.）

Resonant X-ray scattering (Tohoku University)

Youichi Murakami, Hironori Nakao, Tetsuya Murata

Neutron diffraction (Tohoku University)

Kazuyoshi Yamada, Haruhiro Hiraka

Ultrasound measurements (University of Electro-Communications)

Masaru Suzuki, Toshiaki Kobayashi, Kohji Abe, Kichizo Asai

$La_{2-x}Sr_xM\ O_4$ system (M: transition metals)

$La_{2-x}Sr_xCuO_4 \cdots d$ –wave superconductor

$Sr_2RuO_4 \cdots p$-wave superconductor

$La_{2-x}Sr_xNiO_4 \cdots$ charge stripe ordering

$La_{2-x}Sr_xMnO_4 \cdots$ charge and orbital ordering

$La_{2-x}Sr_xCoO_4$ system is expected to show the novel physical properties

Spin state in $La_{2-x}Sr_xCoO_4$

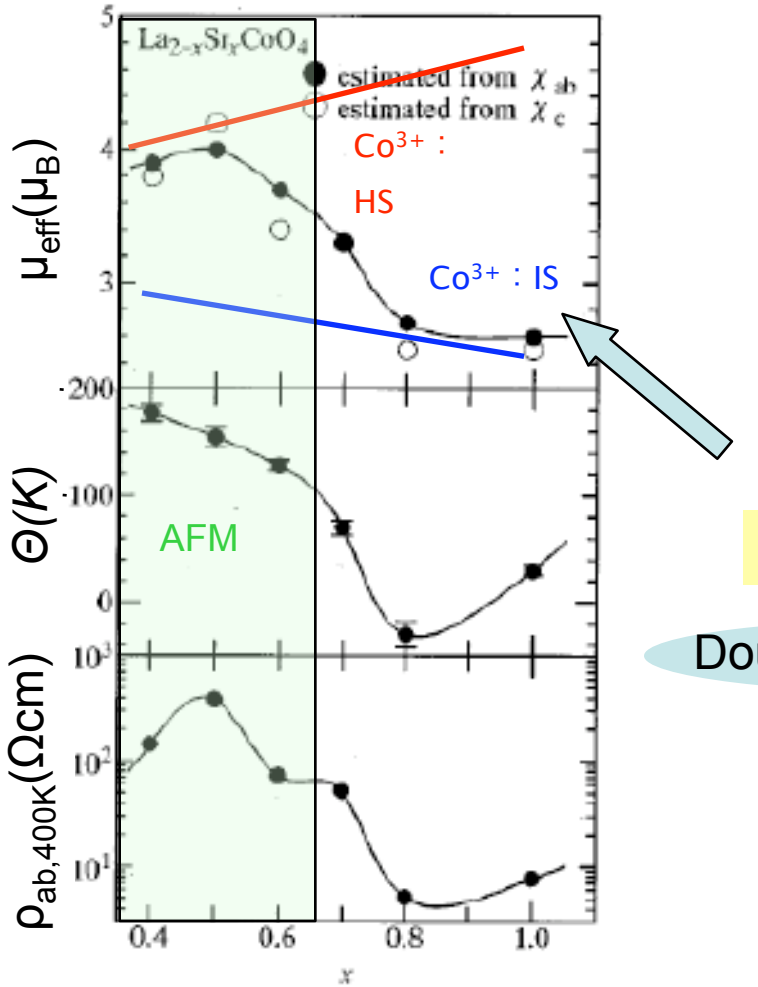

Y. Moritomo *et al.*,
Phys. Rev. B **55**, R14 725 (1997)

Co^{3+} : $(3d)^6$

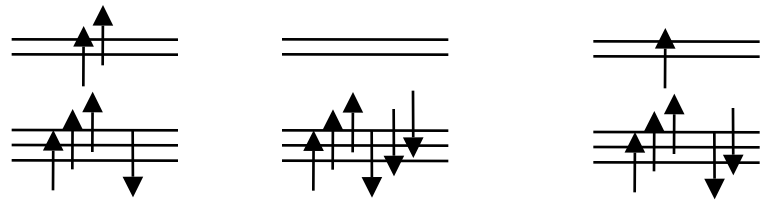

High spin state (HS)	Low spin state (LS)	Intermediate spin state (IS)
S=2(4.89μ_B)	S=0(0μ_B)	S=1(2.83μ_B)

IS state was realized by Sr substitutions!!

Double –exchange model

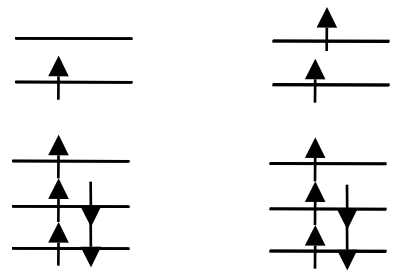

Co^{3+}(IS) Co^{2+}(HS)

Weiss temperature Θ and resistivity ρdecrease by the interaction.

Spin state in $La_{2-x}Sr_xCoO_4$

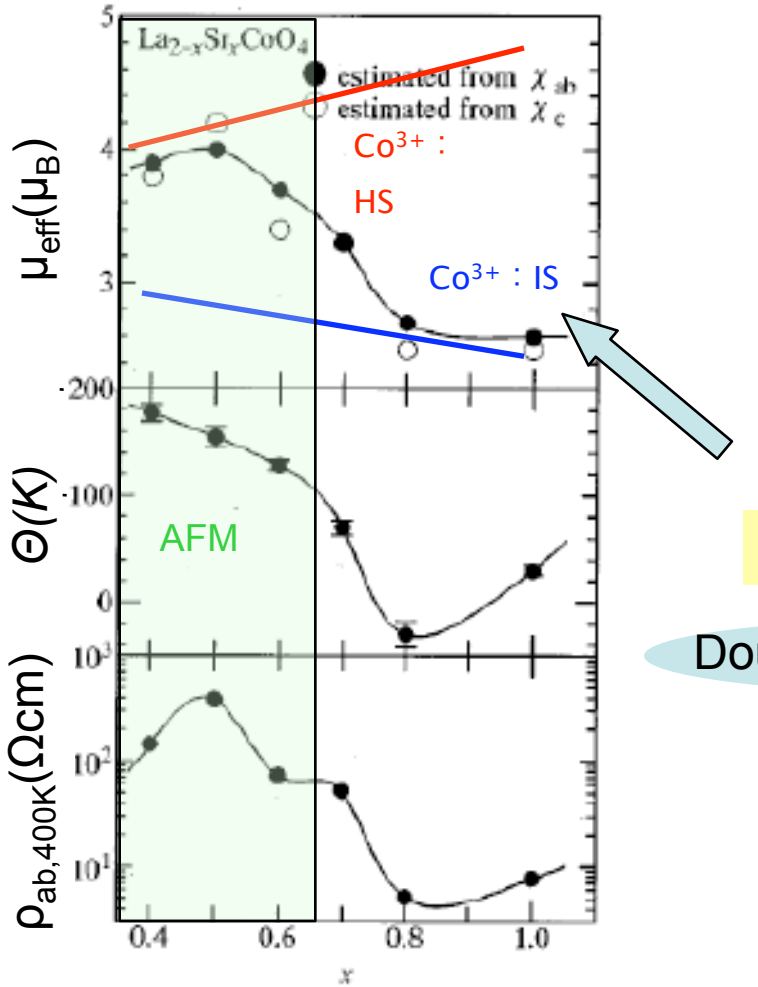

Y. Moritomo *et al.*,
Phys. Rev. B **55**, R14 725 (1997)

Co^{3+} : $(3d)^6$

High spin state (HS)	Low spin state (LS)	Intermediate spin state (IS)
S=2(4.89μ_B)	S=0(0μ_B)	S=1(2.83μ_B)

IS state was realized by Sr substitutions!!

Double –exchange model

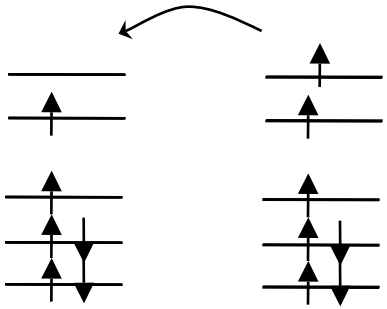

Co^{3+}(IS) Co^{2+}(HS)

Weiss temperature Θ and resistivity ρdecrease by the interaction.

Charge ordering in $La_{2-x}Sr_xCoO_4$

Checkerboard type charge ordering model

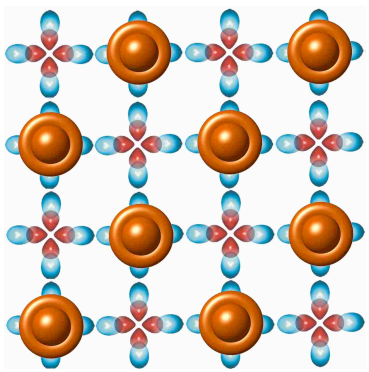

Checkerboard charge ordering.

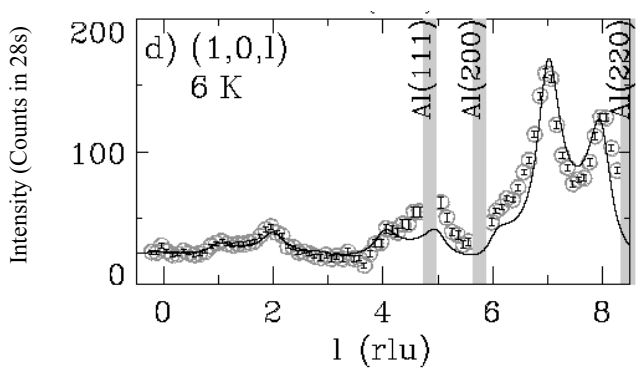

Charge ordering patterns were determined from **diffuse peaks**.

Crystal structure of $La_{1.5}Sr_{0.5}CoO_4$

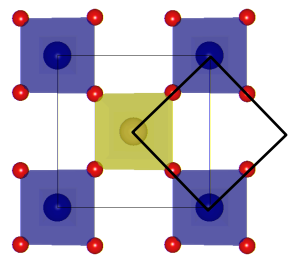

Charge ordered unit cell

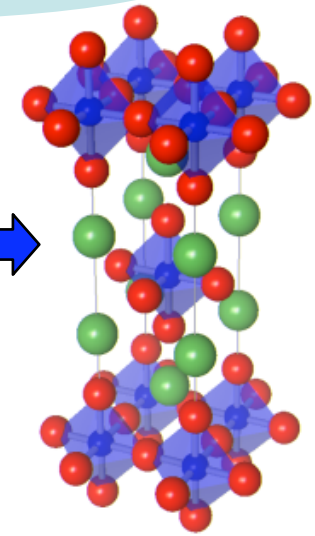

Space group: *I4/mmm*

Checkerboard type charge ordering has not been determined by crystal structural analysis because the diffuse reflections are too weak

Purpose in the present study

Purpose

1. Determine the charge ordered state and its crystal structure
2. Clarify the Intermediate spin state and its origin
3. Determine the magnetic structure and its hole-doping dependence

$La_{2-x}Ca_xCoO_4$ system is best candidate to understand the upper purpose.

1. Spin state transition by controlling the filling in $La_{2-x}Ca_xCoO_4$

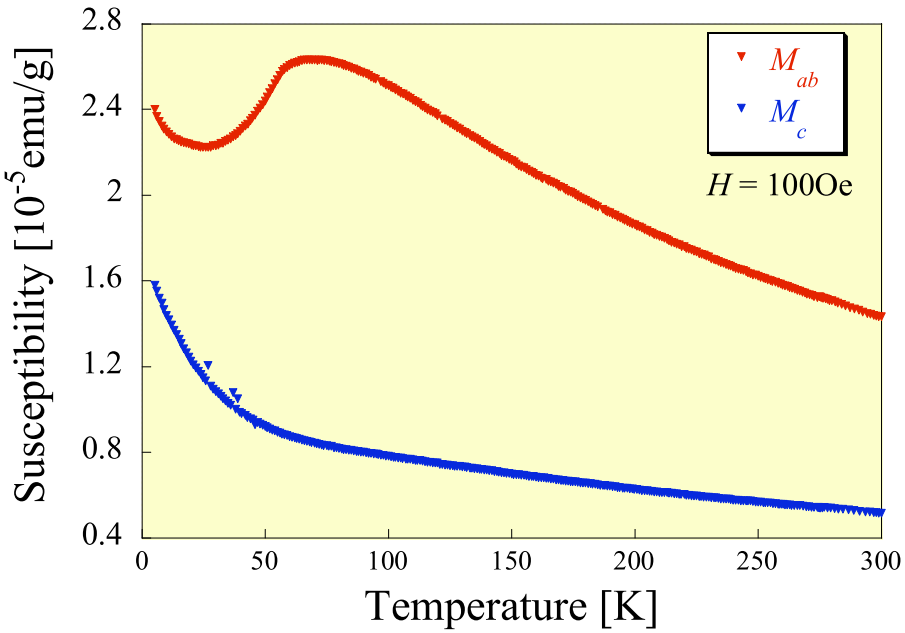

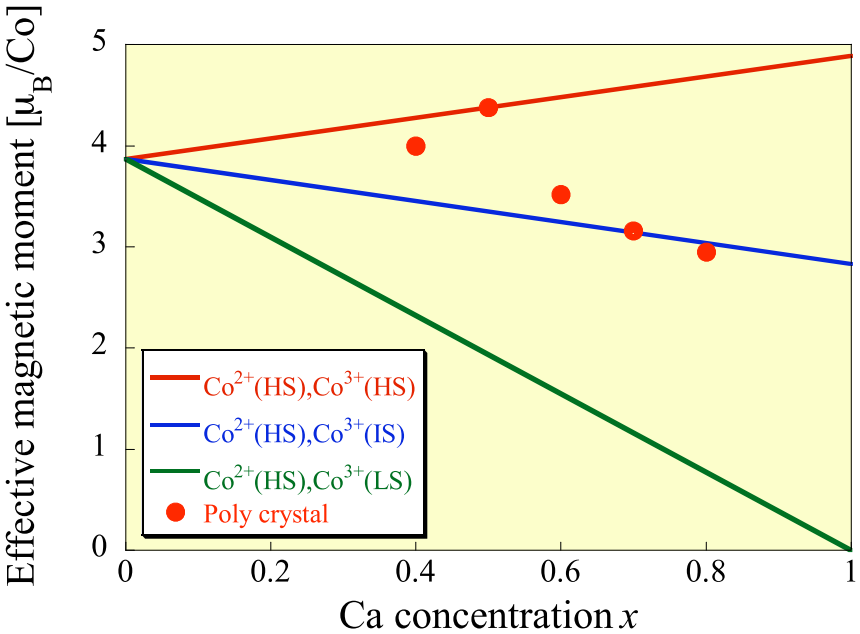

$T_N \sim 50$K

Spin state transition from Co^{3+}(HS) to Co^{3+}(IS) with increasing Ca concentration

§1 Single crystal growth and crystal structure analysis in $La_{2-x}Ca_xCoO_4$

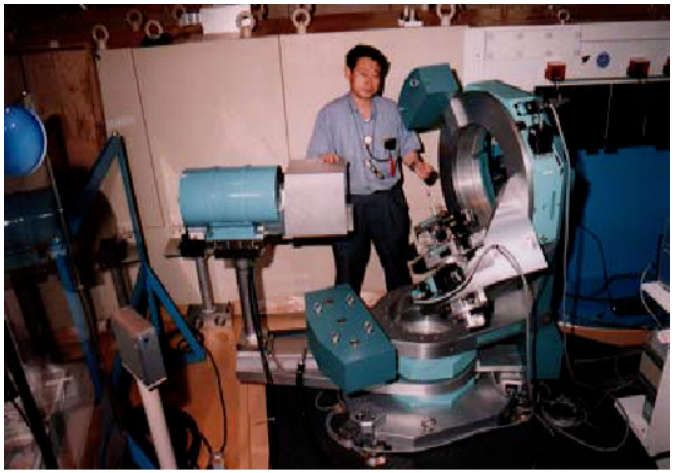

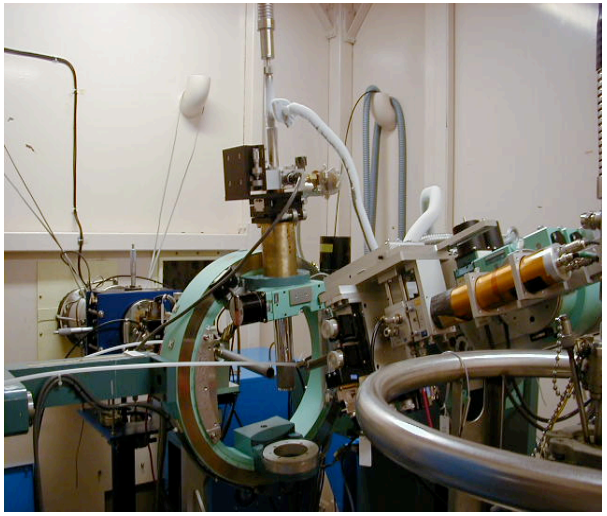

Crystal growth

Single crystal sample

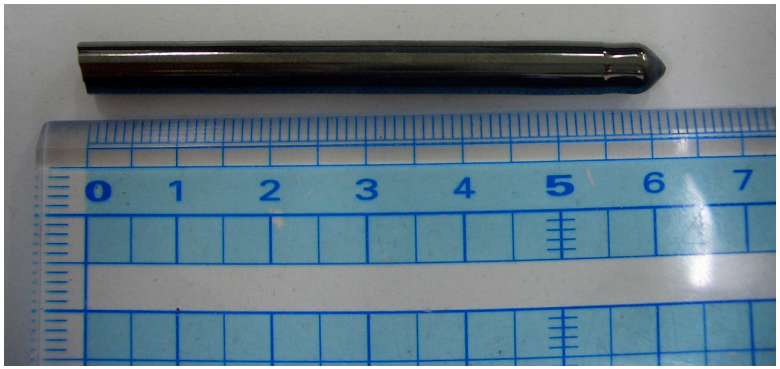

Length: 60mm

Diameter: 5mm

Laue photograph

[001] direction

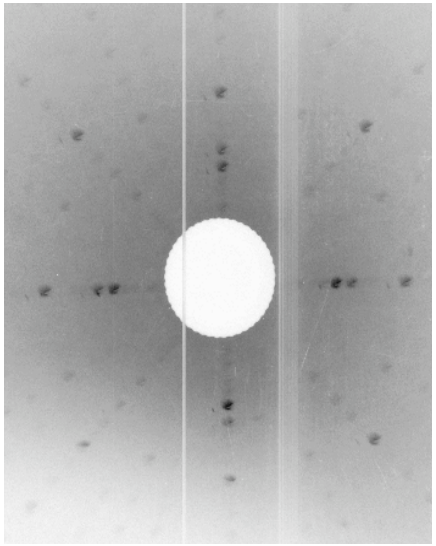

Space group in $La_{1.5}Ca_{0.5}CoO_4$ has been determined to be *Cmm*2(*A*2*mm*) from the convergent electron diffraction.

Analysis results

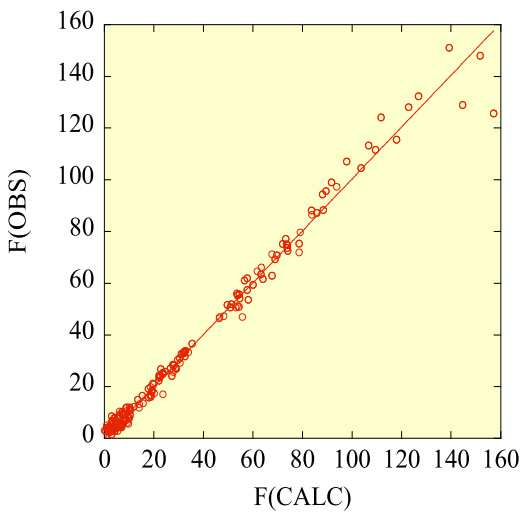

Structural parameters of $La_{1.5}Ca_{0.5}CoO_4$

	x	*y*	*z*	*U*
Co(1)	0	0	0	0.000(3)
Co(2)	0.499(5)	0.5	0	0.000(3)
O(1)	0.247(2)	0.247(2)	0	0.001(1)
O(2)	0.757(2)	0.753(2)	0	0.010(2)
O(3)	0.015(2)	0	0.1654(4)	0.007(1)
O(4)	0.507(2)	0.5	0.1738(5)	0.011(1)
La,Ca(1)	0	0	0.3614(3)	0.002(1)
La,Ca(2)	0	0.5	0.3622(3)	0.001(1)

A2mm (r =0.50), R=6.62, Rw=7.28
a=5.416(4), b=5.404(2), c=12.313(6)
α=90, β=90, γ=90

Two Co site, Co (1) and Co(2), are existed.

Crystal structure of $La_{1.5}Ca_{0.5}CoO_4$

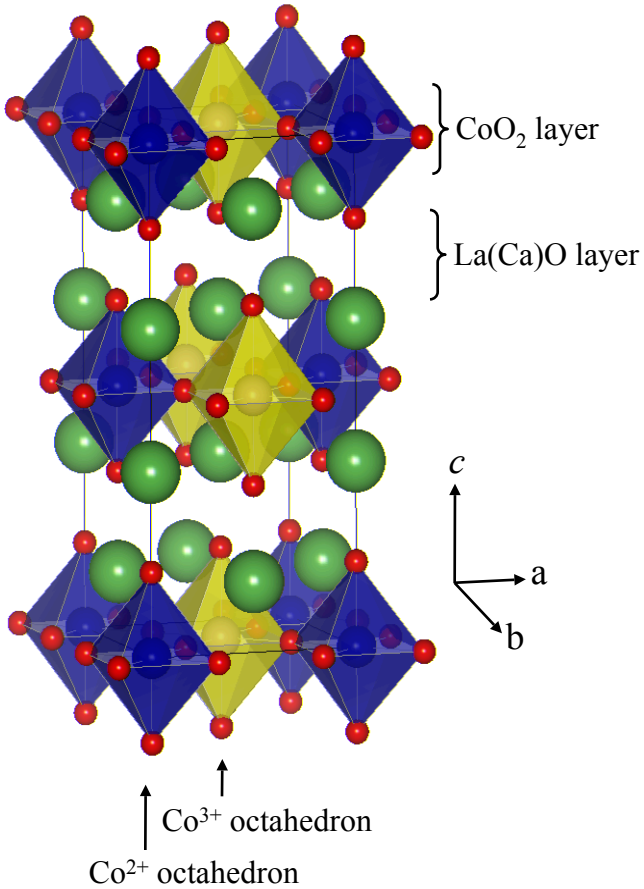

Checkerboard type arrangement

Presumption of Co(1), Co(2) site valences

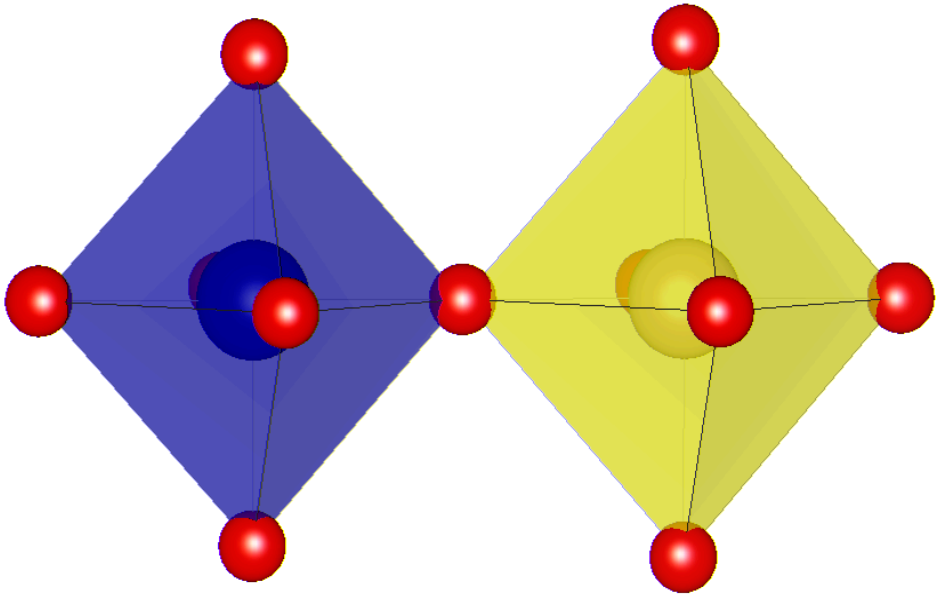

	$Co(1)O_6$	$Co(2)O_6$
Cell volume	**small**	**large**
valence	Co^{3+}	Co^{2+}

Bond length between Co and O

bond	*distance* (Å)
$Co(1)\text{-}O_{in\text{-}plane}$	1.89(2)
$Co(1)\text{-}O_{out\ of\ plane}$	2.039(5)
$Co(2)\text{-}O_{in\text{-}plane}$	1.94(3)
$Co(2)\text{-}O_{out\ of\ plane}$	2.142(6)

We estimate the charge order pattern and valences by **RXS technique**.

Checkerboard model in $La_{1.5}Ca_{0.5}CoO_4$

Checkerboard model

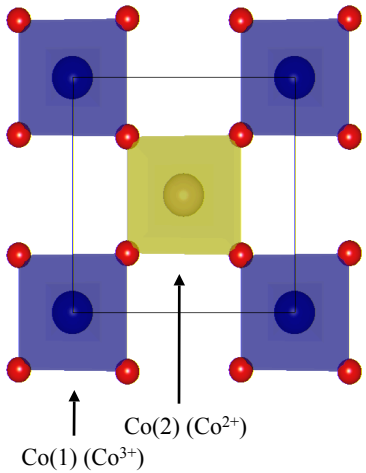

$$f_1 = \frac{1+\delta_c}{2} f(Co^{3+}) + \frac{1-\delta_c}{2} f(Co^{2+})$$

$$f_2 = \frac{1-\delta_c}{2} f(Co^{3+}) + \frac{1+\delta_c}{2} f(Co^{2+})$$

δc: order parameter of charge ordering

δc=1: full charge disproprotration (Co^{2+}/Co^{3+})

δc=0: no charge ordering ($Co^{2.5+}/Co^{2.5+}$)

The structure factor $F(h,0,0)$ (h:odd)

$$F(h,0,0) \propto f_1 - f_2 + C$$

$$= \delta_c [f(Co^{3+}) - f(Co^{2+})] + C$$

C: lattice distortion due to the charge ordering

(1,0,0), (3,0,0) resonant scattering should be observed in a checkerboard charge ordering

Determination of δ_c and checkerboard model

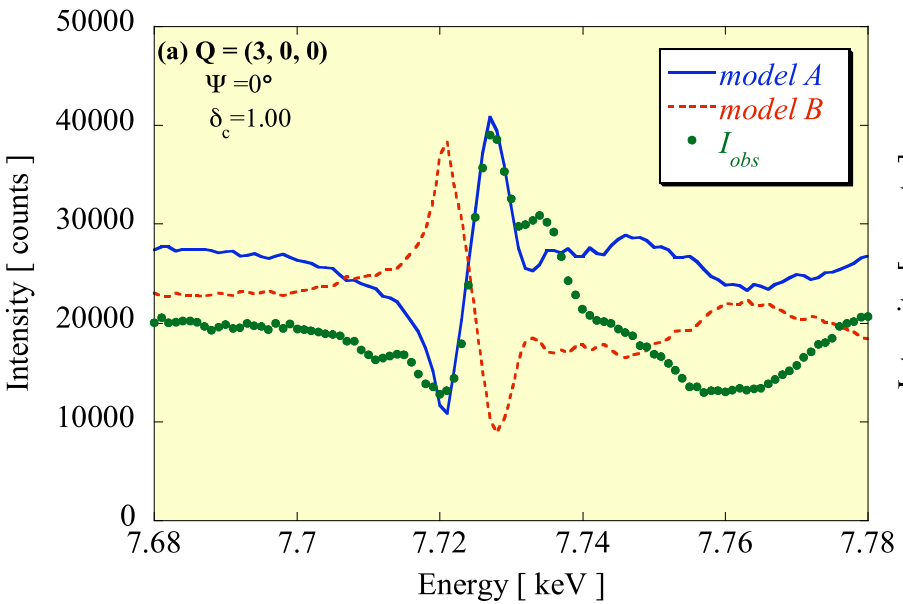

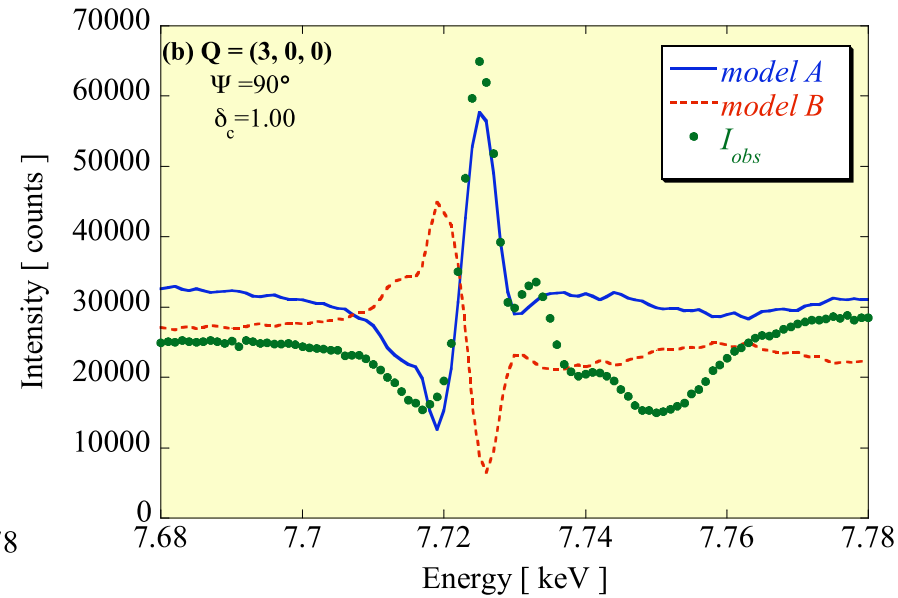

Comparison between

Model A: Co(1)-Co^{3+}, Co(2)-Co^{2+} and **Model B**: Co(1)-Co^{2+}, Co(2)-Co^{3+}

⇨ Full charge disproportionation (**δ_c=1.00(15)**) is realized in the **model A**

Summary

- The crystal structure of $La_{1.5}Ca_{0.5}CoO_4$ was determined to be the ***A2mm*** space group with **twin structure**.

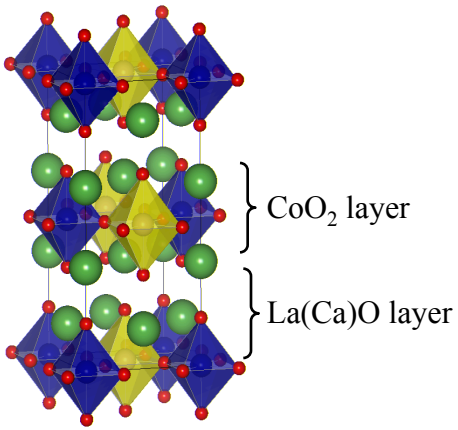

- We found the (3,0,0), (1,0,0) reflections, indicating that the full charge disproportionation was realized in this system

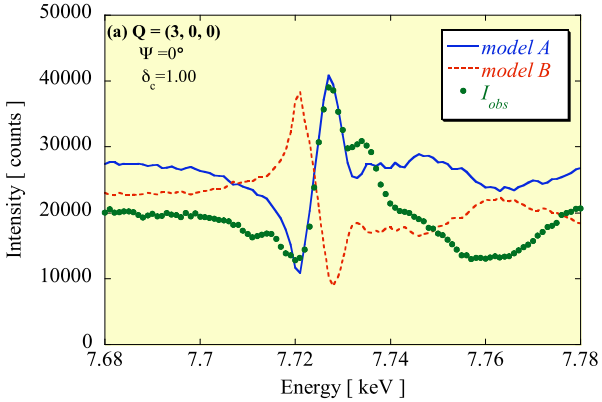

§2

Spin and charge orders and their hole doping dependence in $La_{2-x}Ca_xCoO_4$ ($0.3<x<0.8$) by using neutron diffraction

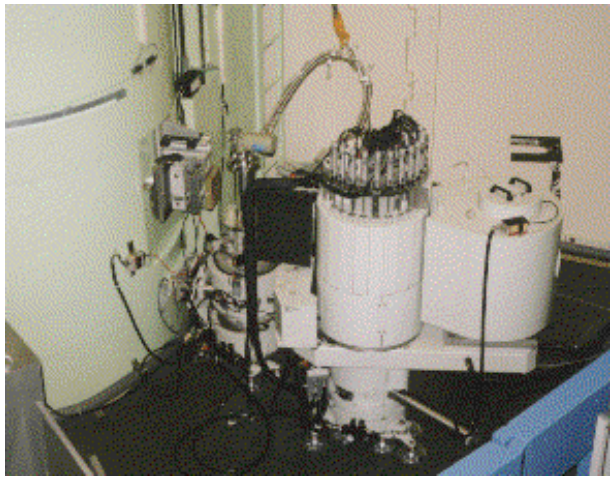

Experimental details

Sample: $La_{2-x}Ca_xCoO_4$ ($0.3<x<0.8$) single crystal
(4mmφ×40.0mm)

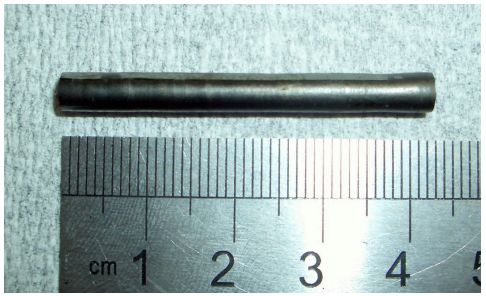

Spectrometer:

TOPAN(6G) monochromator: PG(002)

E_i=30.5meV, collimation: B(50')-30'-S-60'-B(180')

AKANE(T1-2) monochoromator: Ge(3,1,1)

E_i=19.7meV, collimation: g(20')-open-S-60'-B(180')

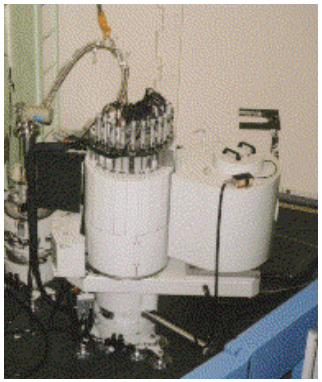

Scattering plane: **(H,0,L), (H,H,L)**

Unit cell: the charge ordered unit cell
(a～b～5.418 Å, c～12.469 Å　(x＝0.5))

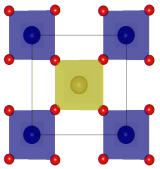

Charge ordering (CO) and spin ordering (SO) in $La_{1.5}Ca_{0.5}CoO_4$

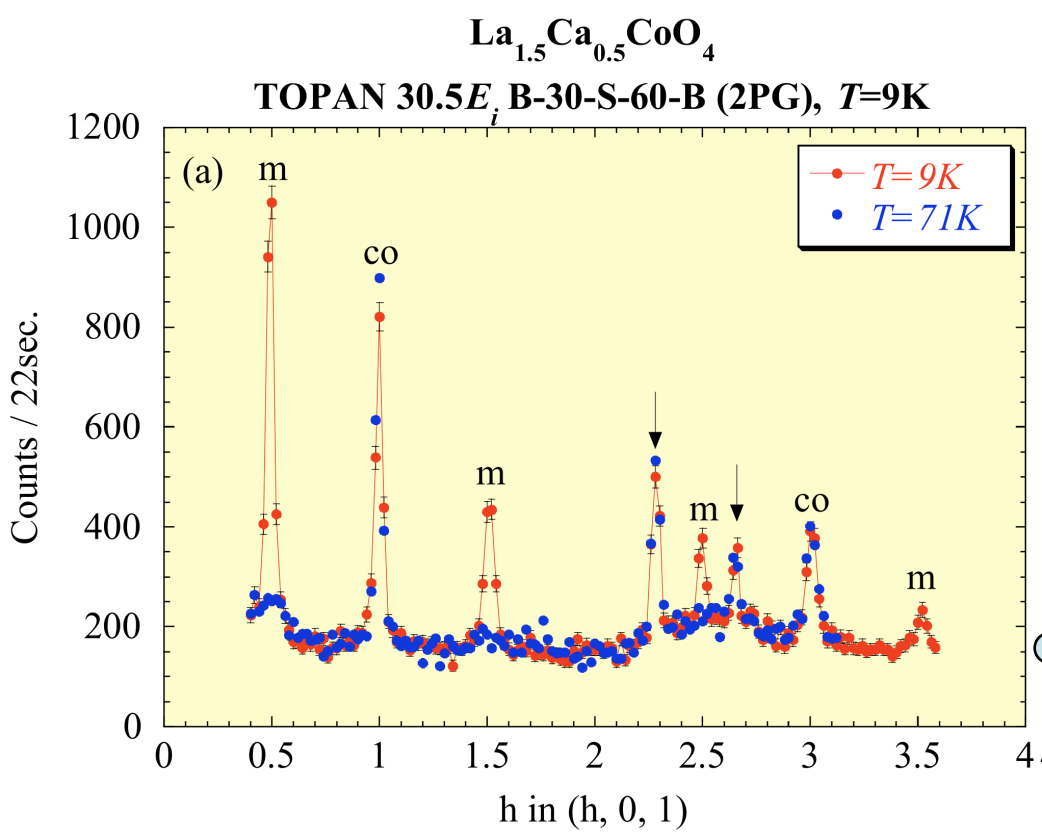

The elastic scattering in the (H0L) reciprocal plane of $La_{1.5}Ca_{0.5}CoO_4$

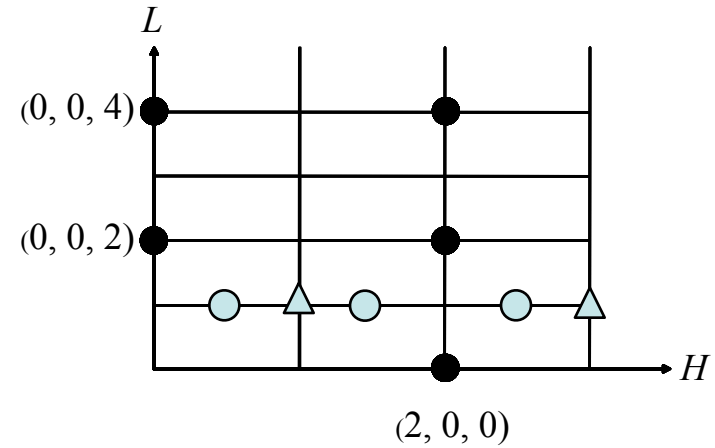

●:nuclear Bragg scattering (NB)

○ Q_m=(**h±0.5**,0,1) (magnetic scattering)

△ Q_{co}=(**2h±1**,0,1) (structural scattering)

By substituting Ca, **strong nuclear scatterings** due to CO were observed

Charge ordering (CO) and spin ordering (SO) in $La_{1.5}Ca_{0.5}CoO_4$

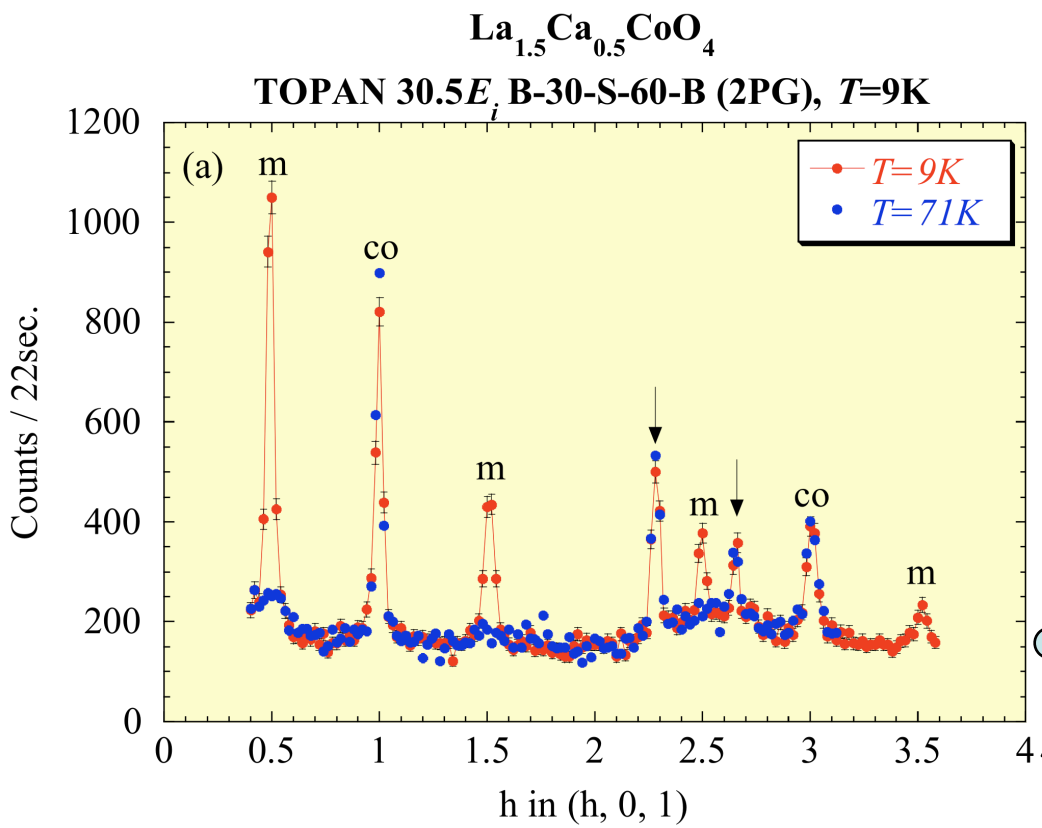

The elastic scattering in the (H0L) reciprocal plane of $La_{1.5}Ca_{0.5}CoO_4$

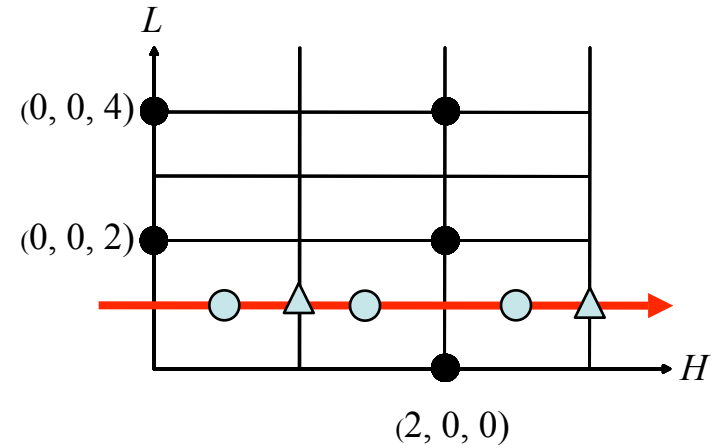

●:nuclear Bragg scattering (NB)

○ Q_m=(h±0.5,0,1) (magnetic scattering)

△ Q_{co}=(2h±1,0,1) (structural scattering)

By substituting Ca, **strong nuclear scatterings** due to CO were observed

Charge ordering in $La_{1.5}Ca_{0.5}CoO_4$

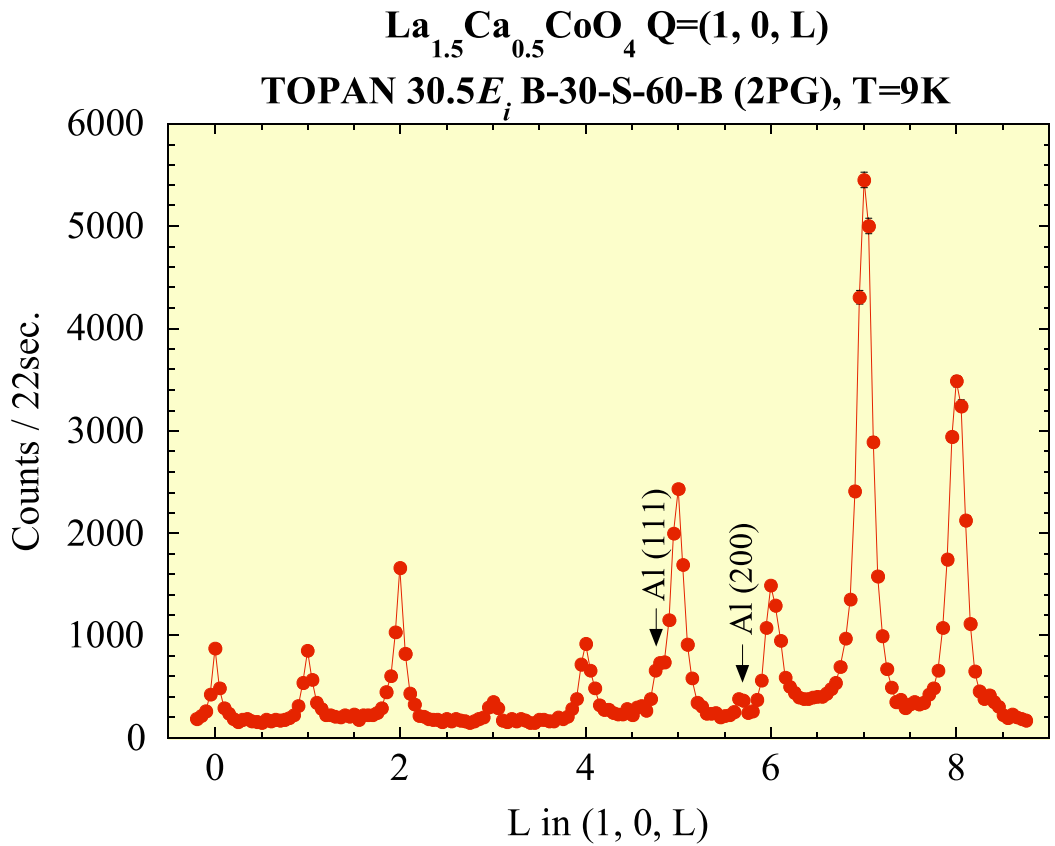

The elastic scattering in the (H0L) reciprocal plane of $La_{1.5}Ca_{0.5}CoO_4$

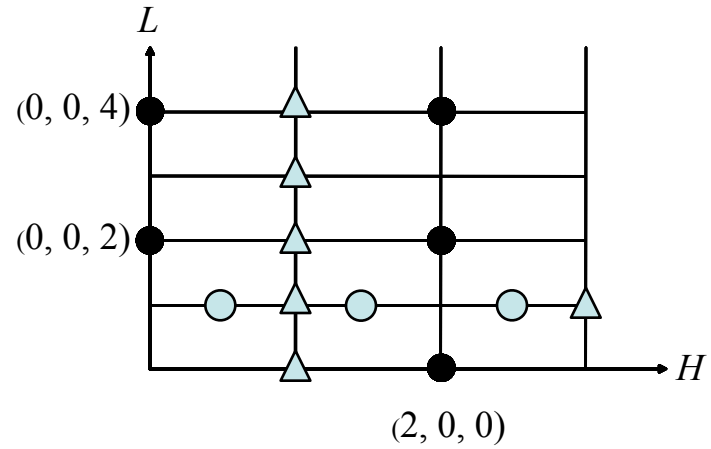

●:nuclear Bragg scattering (NB)

○:magnetic scattering (SO)

△:nuclear scattering due to charge order (CO)

Q_{co}=(2h±1,0,L) (L: integer)

Structural scatterings due to CO were observed at **L=integer** positions.

Charge ordering in $La_{1.5}Ca_{0.5}CoO_4$

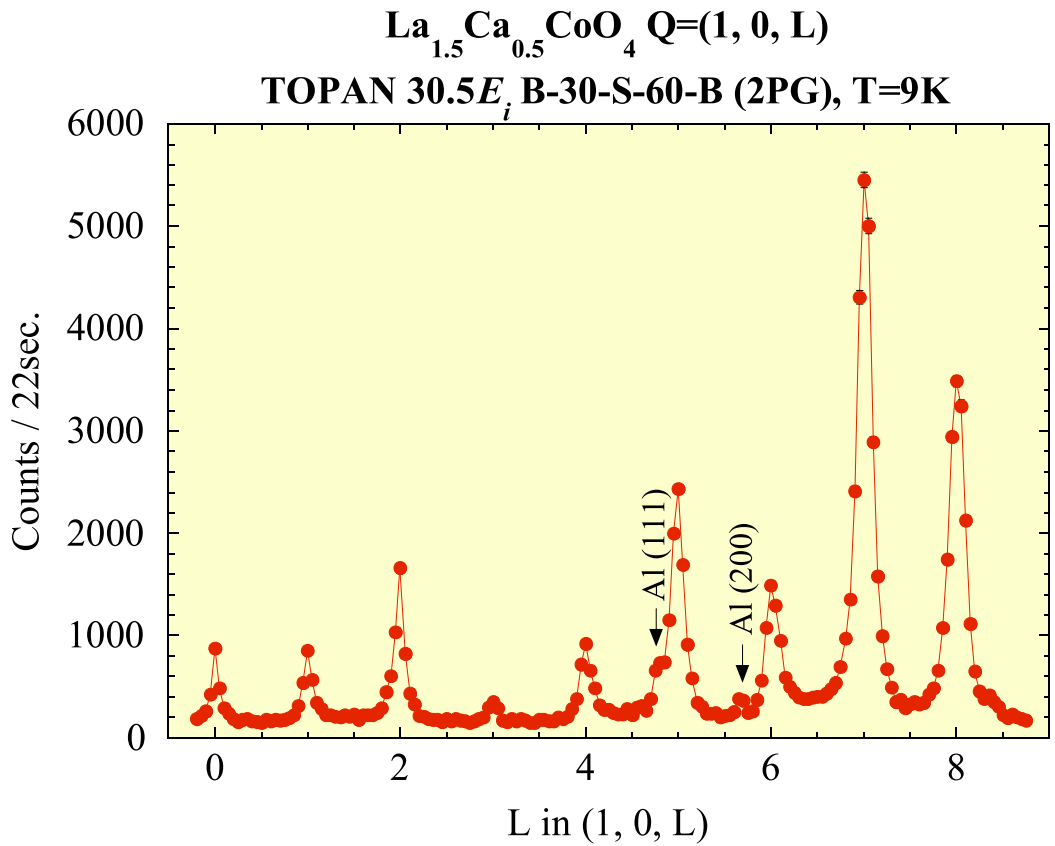

The elastic scattering in the (H0L) reciprocal plane of $La_{1.5}Ca_{0.5}CoO_4$

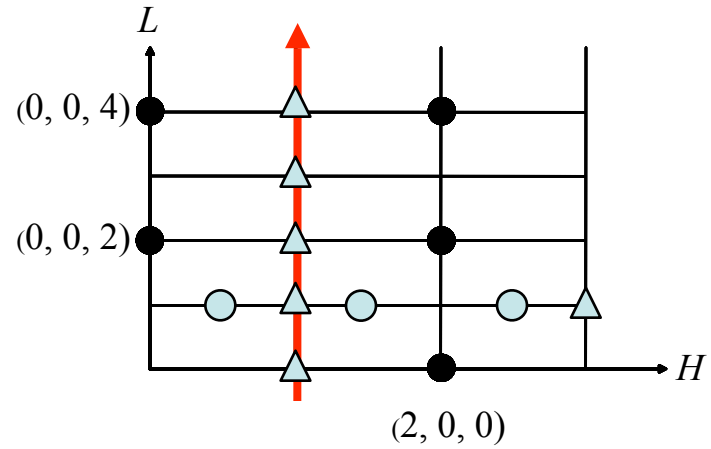

●:nuclear Bragg scattering (NB)

○:magnetic scattering (SO)

△:nuclear scattering due to charge order (CO)

Q_{co}=(2h±1,0,L) (L: integer)

Structural scatterings due to CO were observed at **L=integer** positions.

Charge ordering in $La_{1.5}Ca_{0.5}CoO_4$

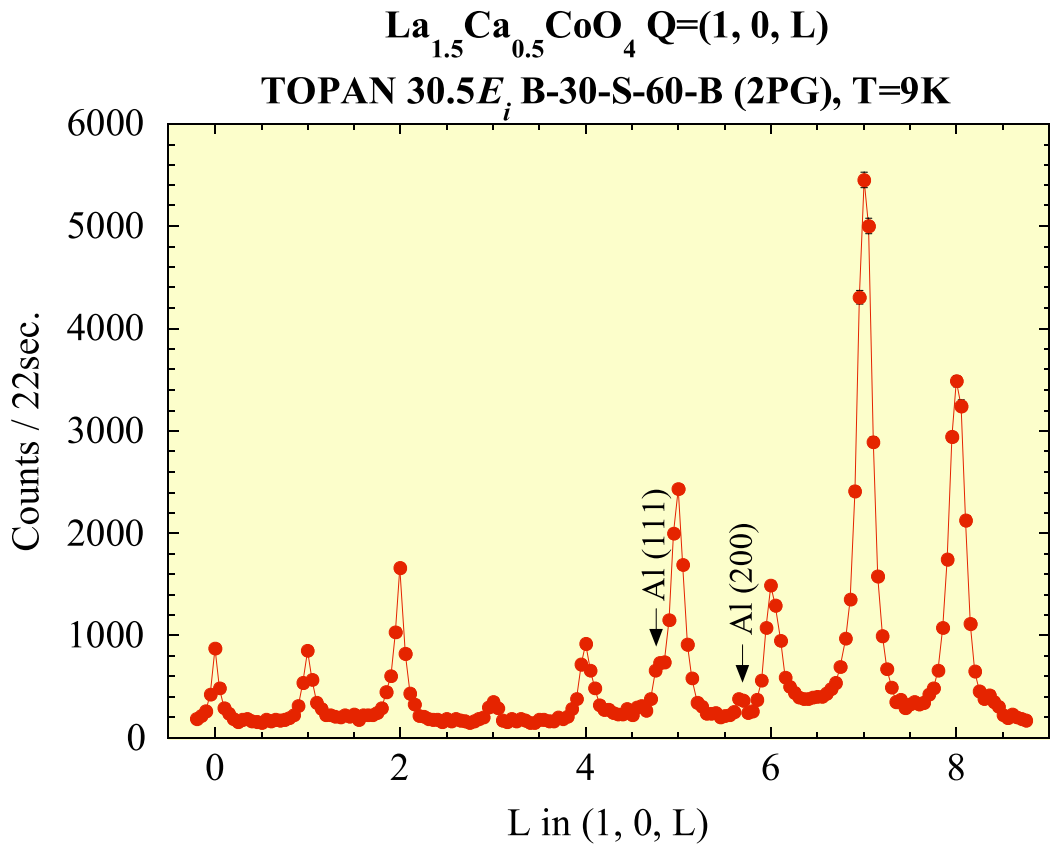

The elastic scattering in the (H0L) reciprocal plane of $La_{1.5}Ca_{0.5}CoO_4$

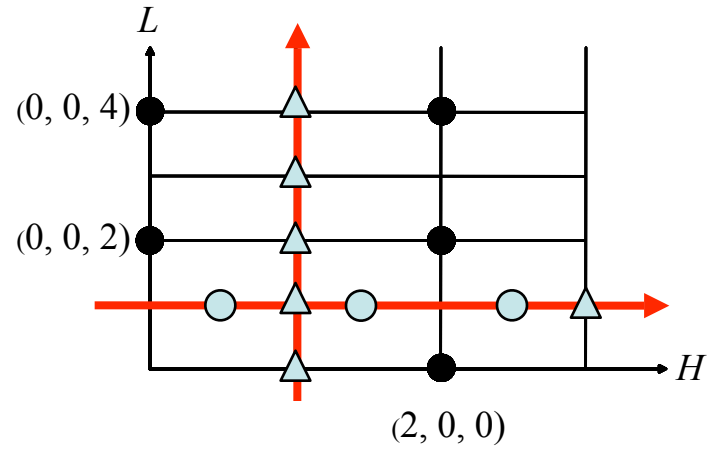

●:nuclear Bragg scattering (NB)

○:magnetic scattering (SO)

△:nuclear scattering due to charge order (CO)

Q_{co}=(2h±1,0,L) (L: integer)

Structural scatterings due to CO were observed at **L=integer** positions.

Charge and magnetic correlation lengths in $La_{1.5}Ca_{0.5}CoO_4$

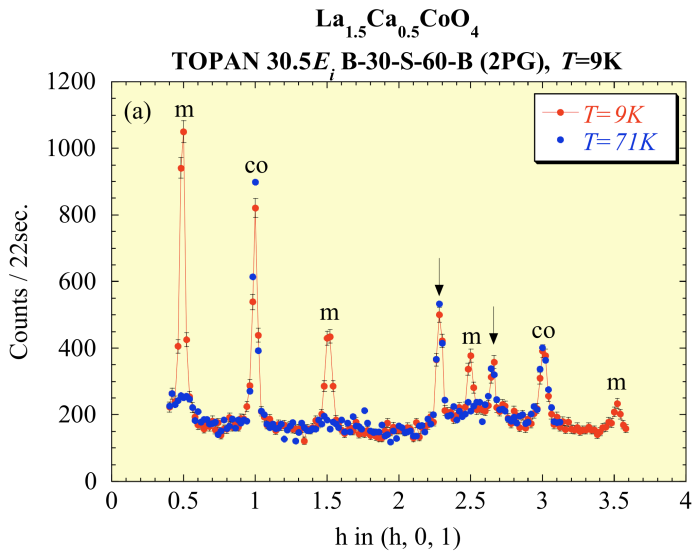

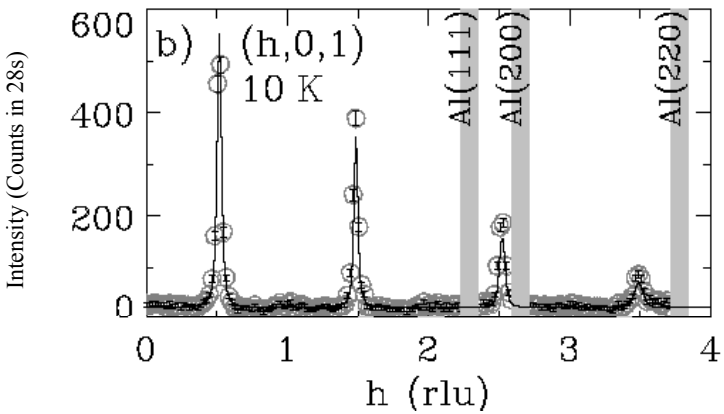

$La_{1.5}Ca_{0.5}CoO_4$

Charge ordering $\xi_{ab(co)}$=**115(12)** Å

$\xi_{c(co)}$ =**59(2)** Å

Magnetic ordering $\xi_{ab(so)}$=98(8) Å

$\xi_{c(so)}$ =11(1) Å

$La_{1.5}Sr_{0.5}CoO_4$

Charge ordering $\xi_{ab(co)}$=**23(2)** Å

$\xi_{c(co)}$ =**8(7)** Å

Magnetic ordering $\xi_{ab(so)}$=79(3) Å

$\xi_{c(so)}$ =10.7(3) Å

CO correlation lengths of Ca system are **five times longer than that of Sr system**

Magnetic scattering along the L direction in $La_{1.5}Ca_{0.5}CoO_4$

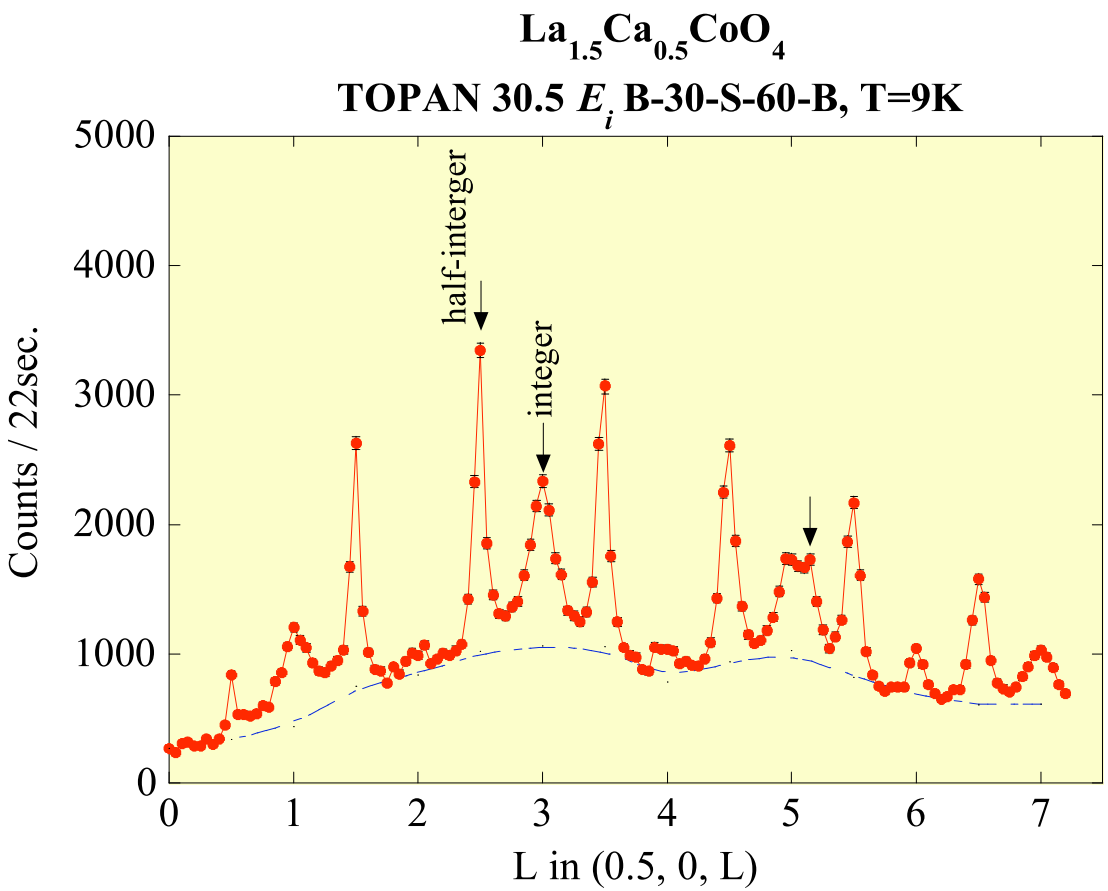

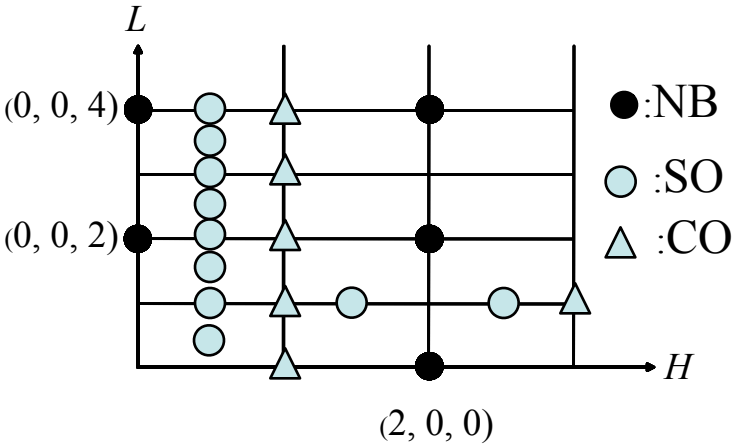

1. Well ordered scattering at **L=half-integer**

ξ_{ab}=195(4) Å, ξ_c=22(1) Å

2. Additional peaks centered at **L=integer**

ξ_{ab}=98(8) Å, ξ_c=11(1) Å

3. Magnetic **diffuse** scattering

We observed **three types of magnetic peaks** in half-doped cobalt system

Magnetic scattering along the L direction in $La_{1.5}Ca_{0.5}CoO_4$

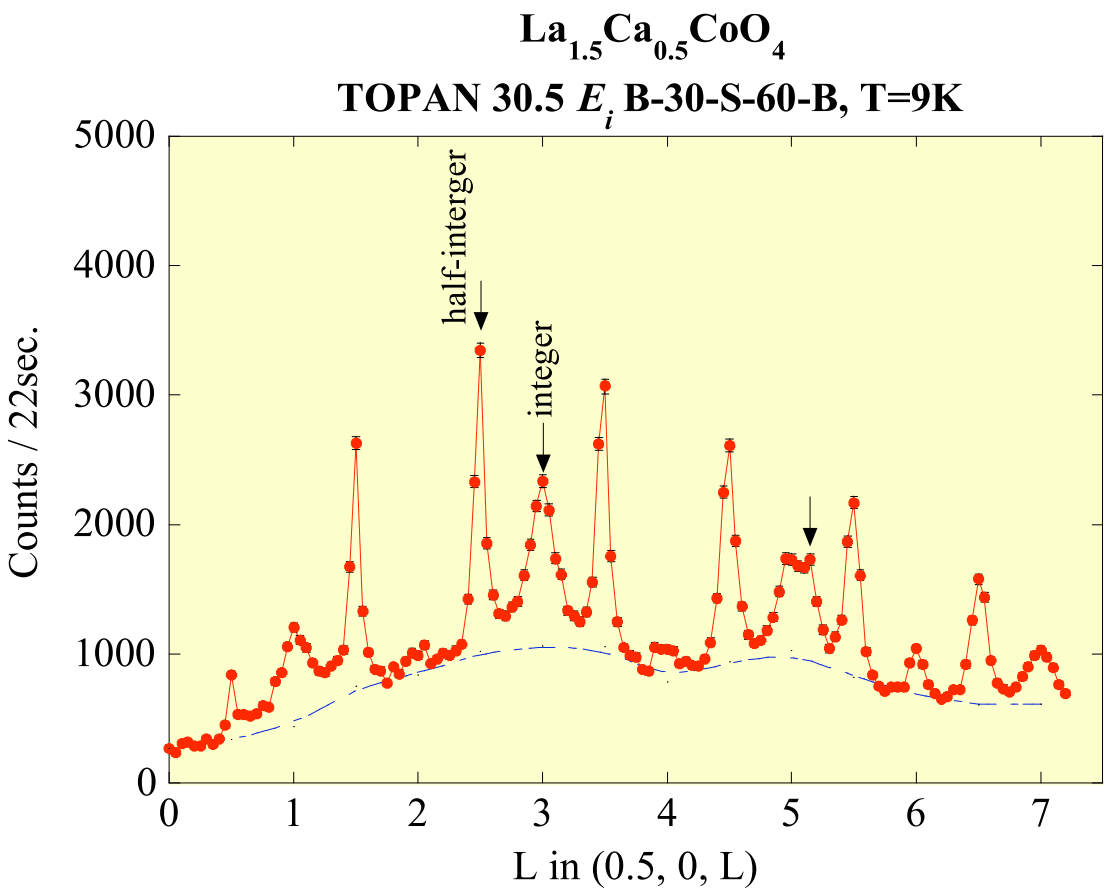

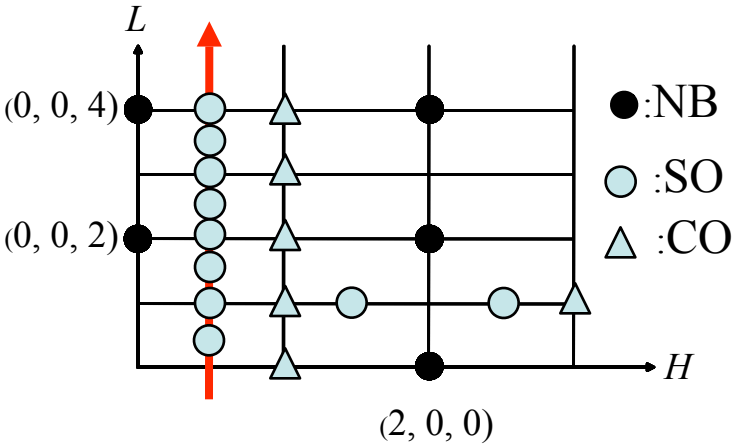

1. Well ordered scattering at **L=half-integer**

ξ_{ab}=195(4) Å, ξ_c=22(1) Å

2. Additional peaks centered at **L=integer**

ξ_{ab}=98(8) Å, ξ_c=11(1) Å

3. Magnetic **diffuse** scattering

We observed **three types of magnetic peaks** in half-doped cobalt system

Summary : magnetic and charge orderings in $La_{1.5}Ca_{0.5}CoO_4$

The elastic scattering in the (H0L) reciprocal plane of $La_{1.5}Ca_{0.5}CoO_4$

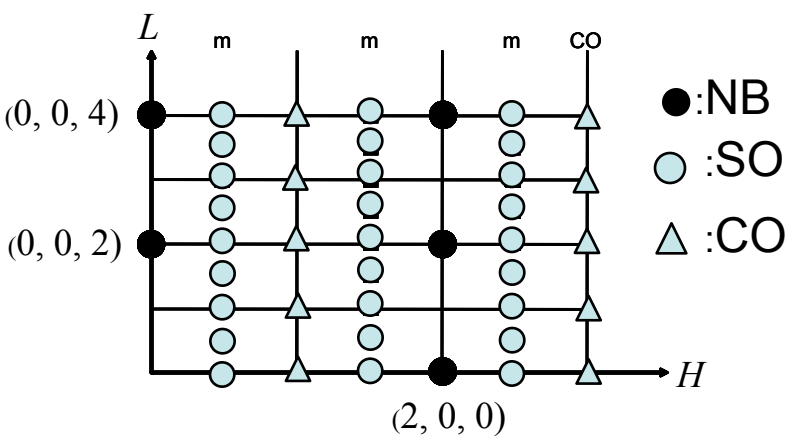

Correlation lengths in half-doped materials

Materials	ξ (CO)_ab	ξ (CO)_c	l=half-integer ξ (SO)_ab	ξ (SO)_c	l=integer ξ (SO)_ab	ξ (SO)_c
$La_{1.5}Ca_{0.5}CoO_4$	115(12)	59(2)	195(4)	22(1)	98(8)	22(1)
$La_{0.5}Sr_{1.5}MnO_4$	>300	~50	>300	~33		
$La_{1.5}Sr_{0.5}CoO_4$	23	8.3(6)			79(3)	10.7(3)
$La_{1.5}Sr_{0.5}NiO_4$	30(10)	2(1)			~120	~13

The origin of the two types magnetic reflections

Magnetic peaks depend on the **stacking patterns along the *c* axis**.

Magnetic scattering in $La_{1-x}Sr_{1+x}MnO_4$

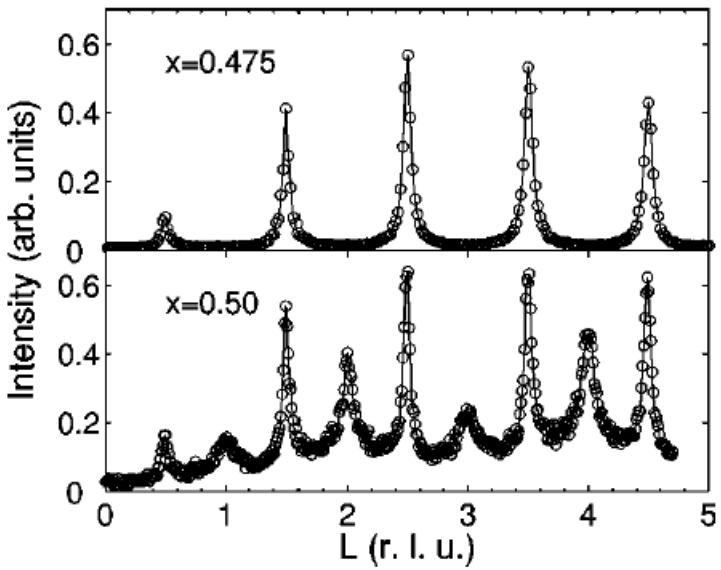

S. Larochelle *et al.*,
Phys. Rev. B **71**, 024435 (2005)

Charge and spin stacking pattern along the *c* axis.

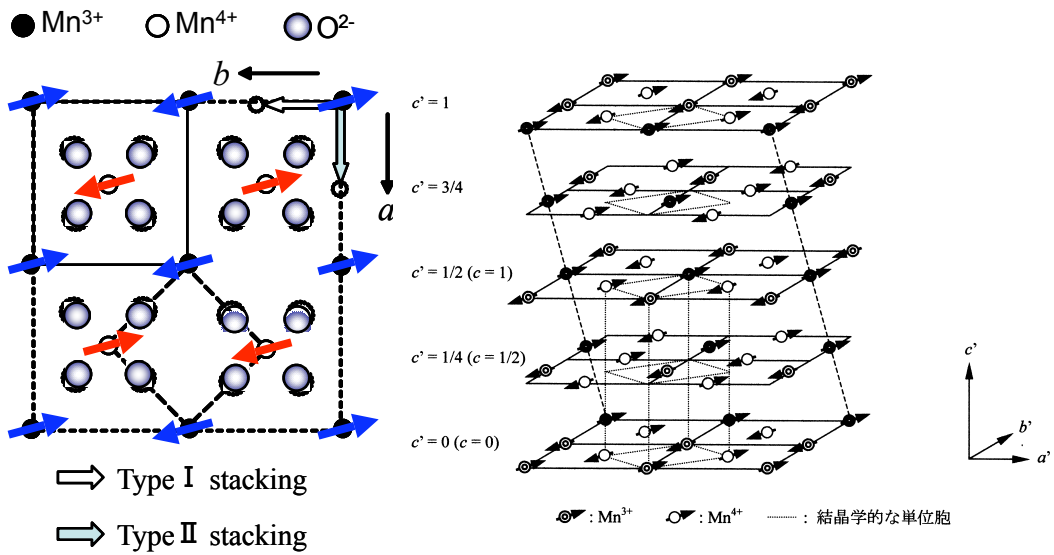

Magnetic scattering origin in $La_{1.5}Ca_{0.5}CoO_4$

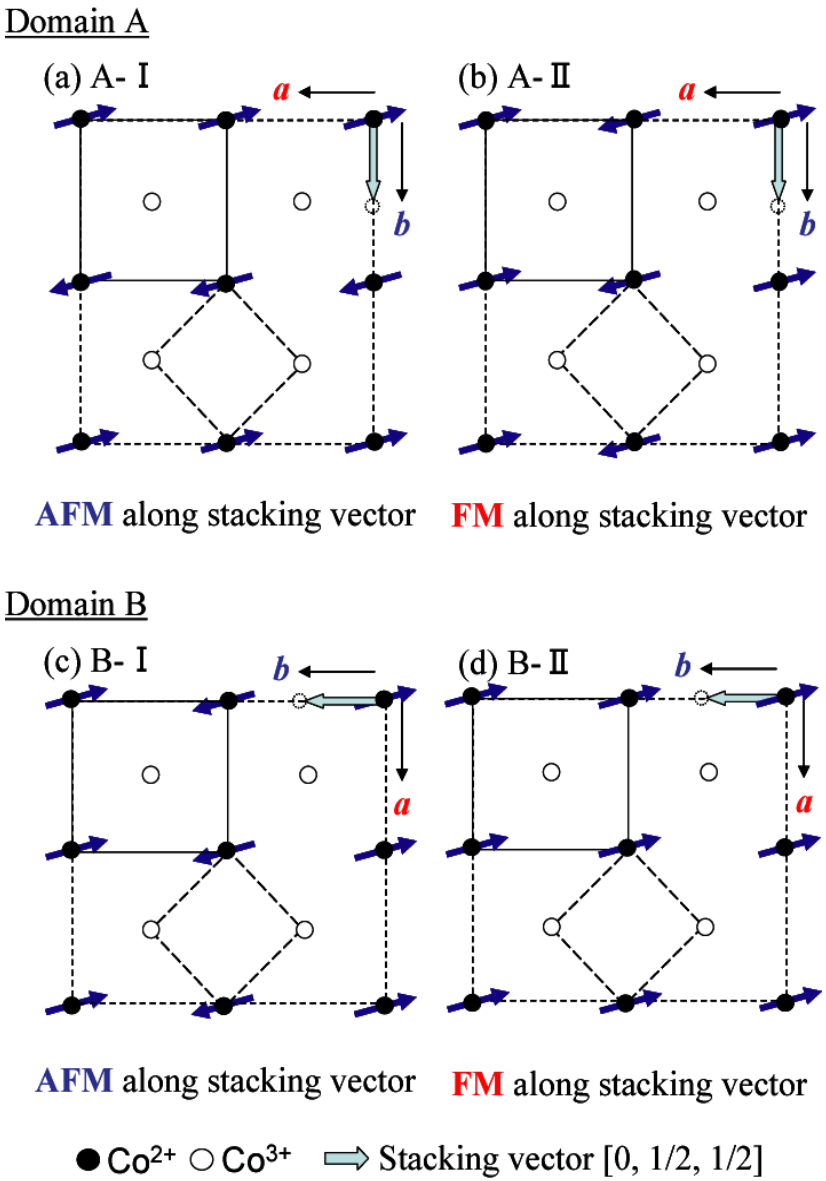

Freedom of **charge** arrangement **2**

Freedom of **spin** arrangement **2**

⇨ **4 magnetic domains** are expected

Domain A $(h, 0, L)_{ortho}$

A- Ⅰ q=(0,1/2,1/2) ⟶ ×

A- Ⅱ q=(1/2,0,0) ⟶ ○

Domain B $(0, k, L)_{ortho}$

B- Ⅰ q=(0,1/2,1/2) ⟶ ○

B- Ⅱ q=(1/2,0,0) ⟶ ×

Magnetic scatterings can be explained by considering the **two magnetic domains**.

Comparison between the calculated and observed magnetic scatterings

peak position	I_{cal}	I_{obs}	$r \cdot I_{cal}$	$(0.5-r) \cdot I_{cal}$
(0.5, 0, 1)	268.3	58.5		49.6
(1.5, 0, 1)	188.0	35.6		34.8
(2.5, 0, 1)	104.1	15.6		19.3
(3.5, 0, 1)	48.6	6.4		9.0
(0.5, 0, 2.5)	341.5	93.6	107.6	
(1.5, 0, 2.5)	196.3	47.5	61.8	
(2.5, 0, 2.5)	100.7	35.5	31.7	
(0.5, 0, 3)	323.3	62.1		59.8
(1.5, 0, 3)	192.3	32.3		35.6
(2.5, 0, 3)	97.8	18.3		18.1
(0.5, 0, 4)	273.3	44.9		50.6
(2.5, 0, 4)	173.6	38.2		32.1
(3.5, 0, 4)	72.0	6.2		13.3

$\mu_{Co}{}^{2+}$=2.86(19), Φs=48°, r(type- I)=0.315

Φs: angle between the spins and the (h,0,0) axis.

The observed magnetic reflections represent as

$$I_{obs} = r_{B-I} \times I_{cal}(type-I) + r_{A-\mathrm{II}} \times I_{cal}(type-\mathrm{II})$$

$$r(A-\mathrm{II}) = 0.5 - r(B-I)$$

- We estimated the ratio of r(type-I)=0.315

  ⇨ **type-I stacking** is majority

- Magnetic moment μ_{Co2+}=2.86(19)μ_B

  ⇨ **Co^{2+}(HS)** is realized in x=0.5 system.

We qualitatively determine the magnetic structure of Co^{2+} spins

Magnetic scatterings due to Co^{3+} spins

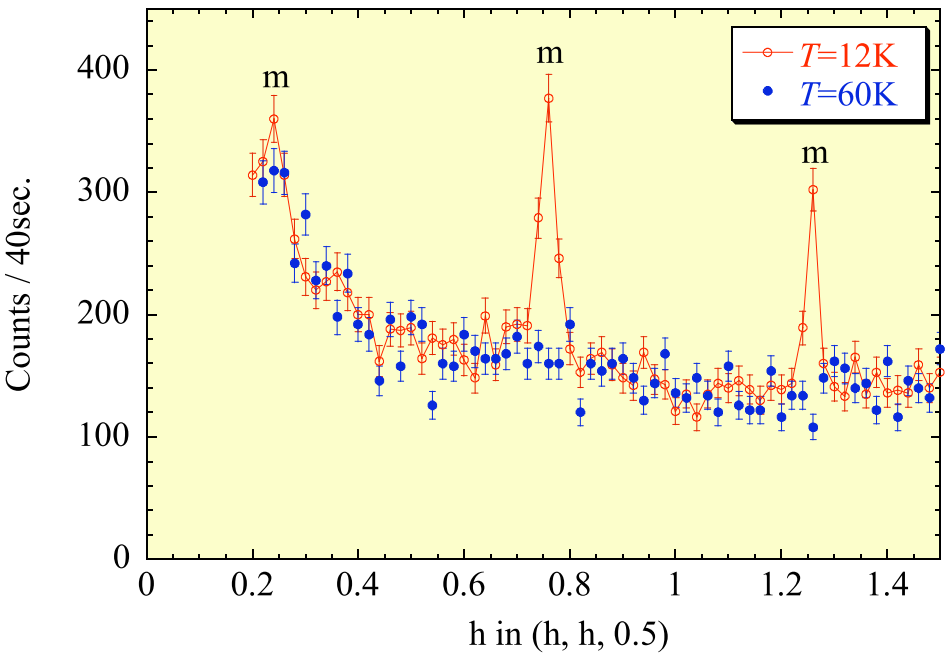

The elastic scattering in the (HHL) reciprocal plane of $La_{1.5}Ca_{0.5}CoO_4$

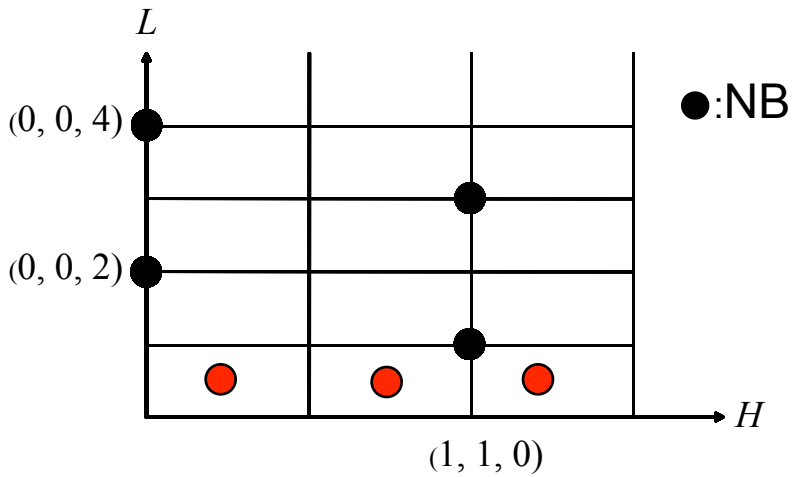

New magnetic scattering

$$Q_m = \left(\frac{2n+1}{4}, \frac{2n+1}{4}, \frac{2m+1}{2}\right)$$

The presence of **(¼, ¼, ½)** indicates that the magnetic unit cell has dimensions **$4a \times 4a \times 2c$** relative to the CO unit cell.

Magnetic scatterings due to Co^{3+} spins

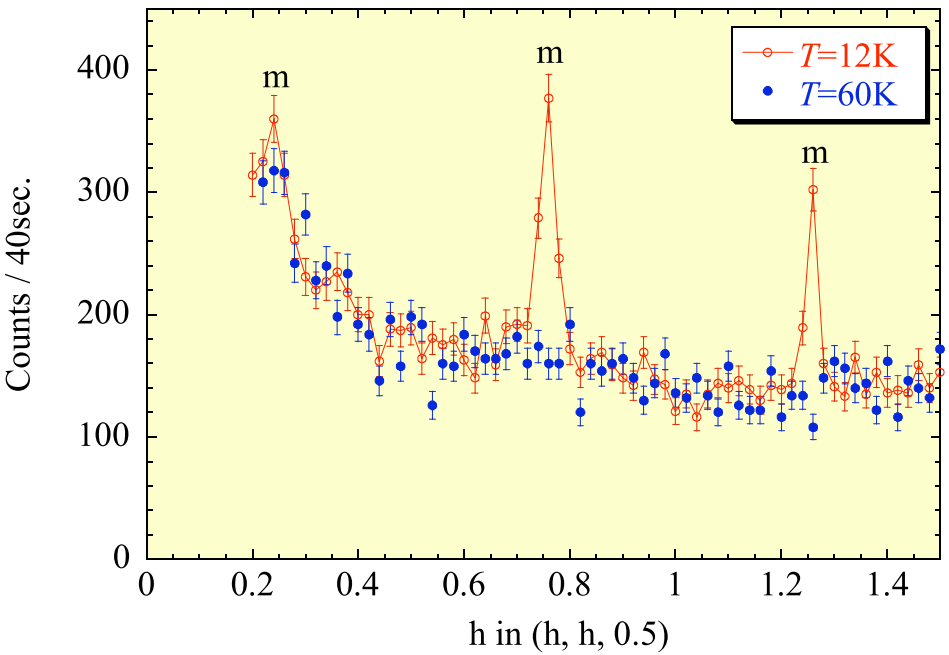

The elastic scattering in the (HHL) reciprocal plane of $La_{1.5}Ca_{0.5}CoO_4$

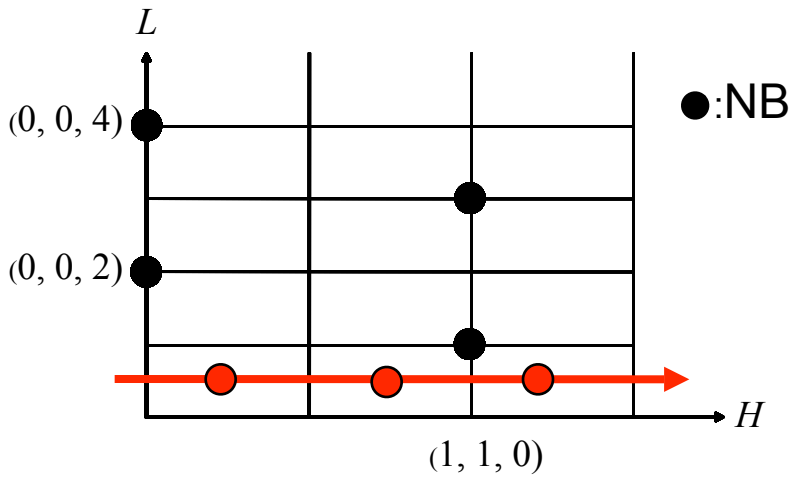

New magnetic scattering

$$Q_m = \left(\frac{2n+1}{4}, \frac{2n+1}{4}, \frac{2m+1}{2}\right)$$

The presence of **(¼, ¼, ½)** indicates that the magnetic unit cell has dimensions **$4a \times 4a \times 2c$** relative to the CO unit cell.

Magnetic scatterings due to Co^{3+} spins

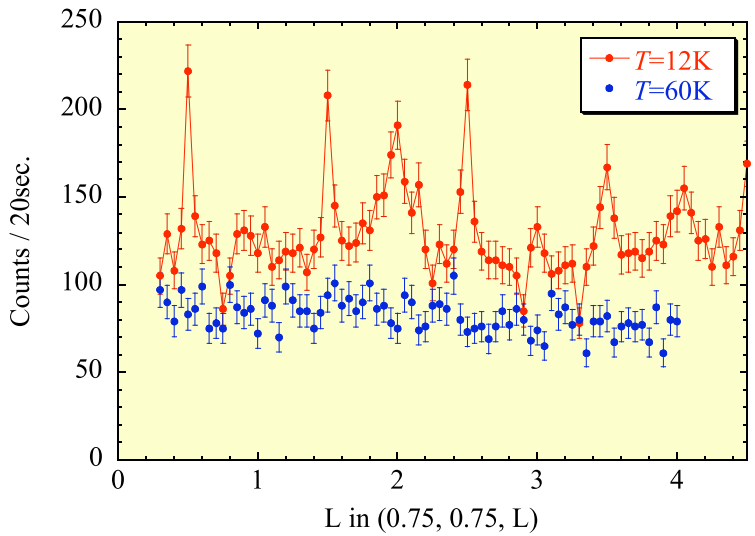

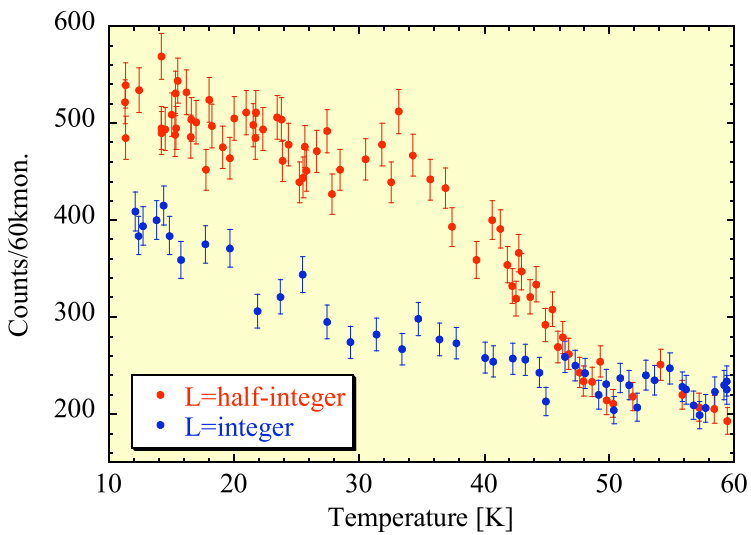

The elastic scattering in the (HHL) reciprocal plane of $La_{1.5}Ca_{0.5}CoO_4$

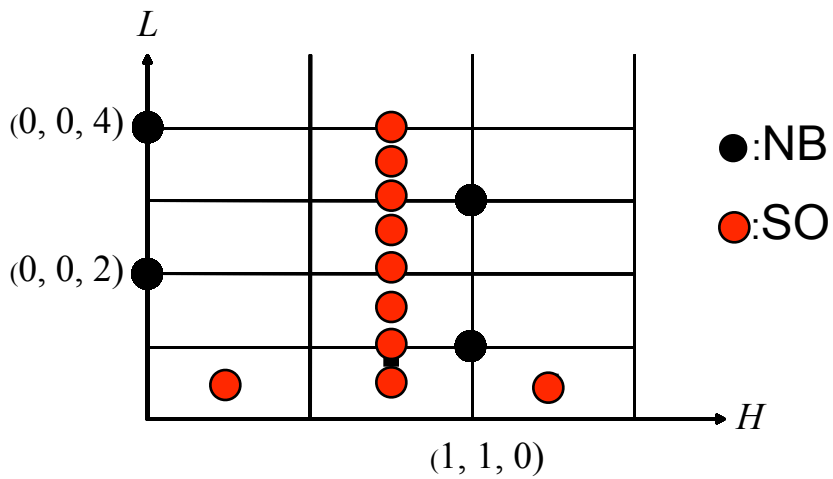

Two types of magnetic scatterings were observed.

1. magnetic peaks at **L=half-integer**, ξab=93(8) Å
2. magnetic peaks at **L=integer** , ξab=74(4) Å

We should take stacking pattern into account

Magnetic scatterings due to Co^{3+} spins

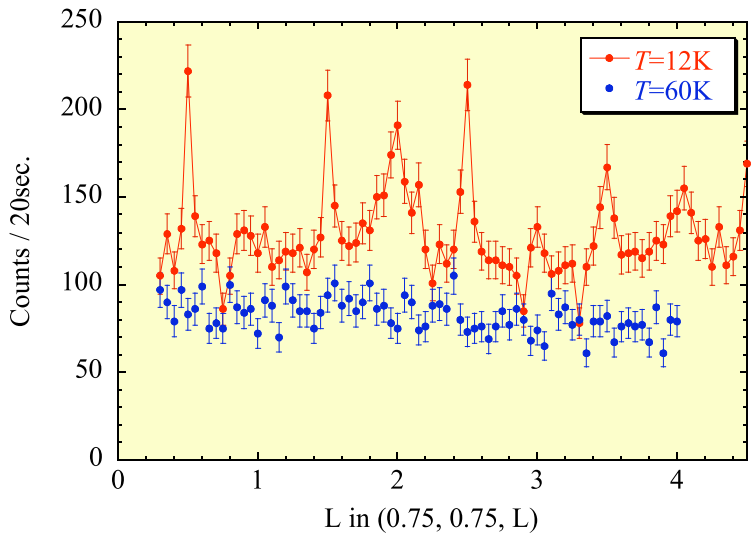

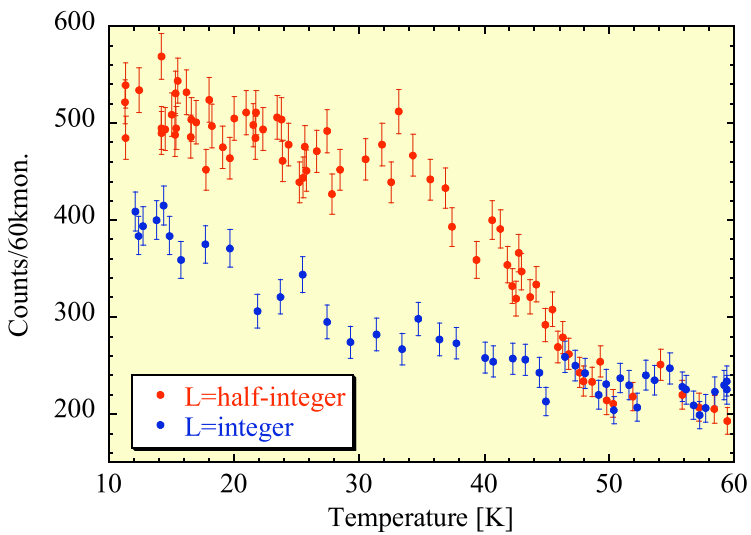

The elastic scattering in the (HHL) reciprocal plane of $La_{1.5}Ca_{0.5}CoO_4$

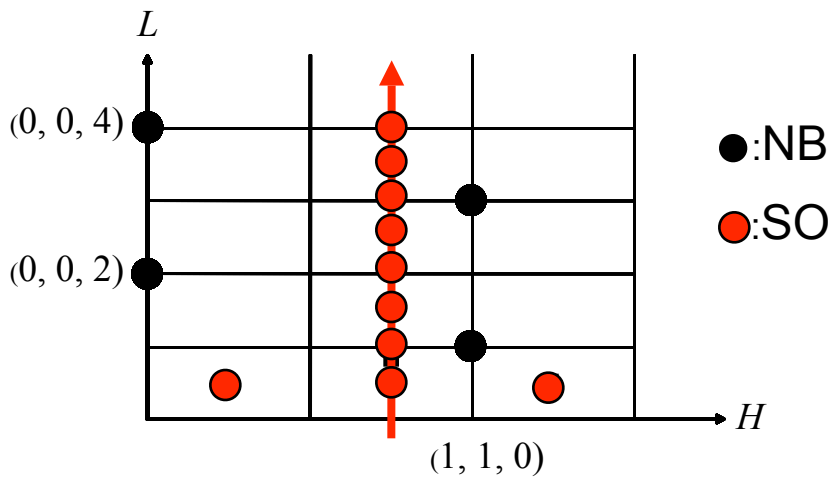

Two types of magnetic scatterings were observed.

1. magnetic peaks at **L=half-integer**, ξab=93(8) Å
2. magnetic peaks at **L=integer** , ξab=74(4) Å

We should take stacking pattern into account

Magnetic scatterings due to Co^{3+} spins

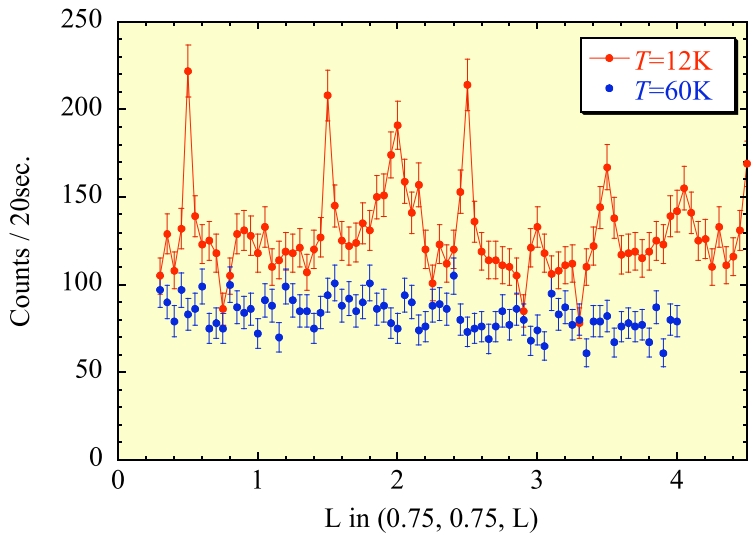

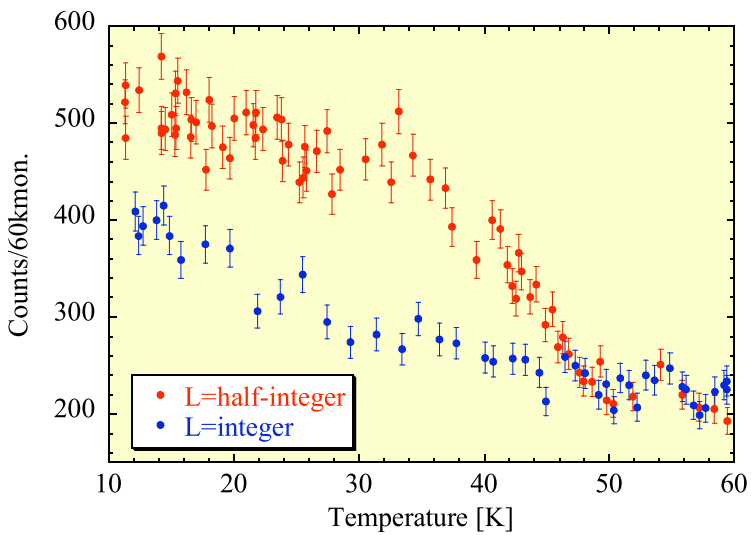

The elastic scattering in the (HHL) reciprocal plane of $La_{1.5}Ca_{0.5}CoO_4$

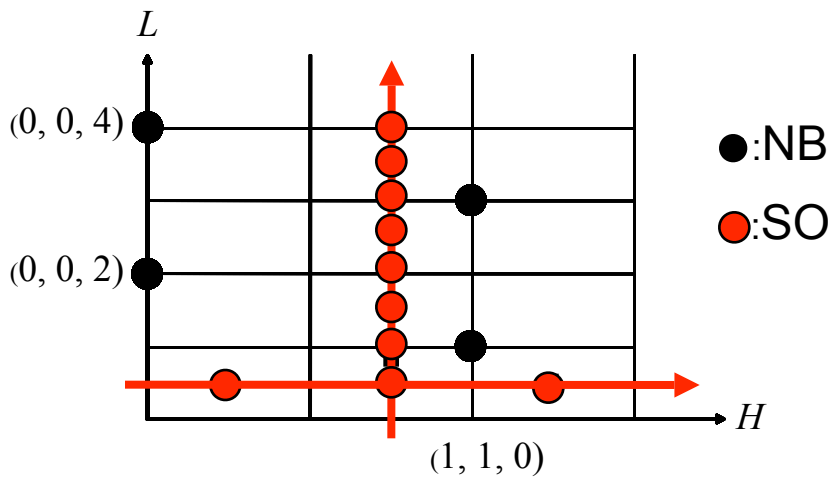

Two types of magnetic scatterings were observed.

1. magnetic peaks at **L=half-integer**, ξab=93(8) Å
2. magnetic peaks at **L=integer** , ξab=74(4) Å

We should take stacking pattern into account

Magnetic scatterings due to Co^{3+} spins

The elastic scattering in the (HHL) reciprocal plane of $La_{1.5}Ca_{0.5}CoO_4$

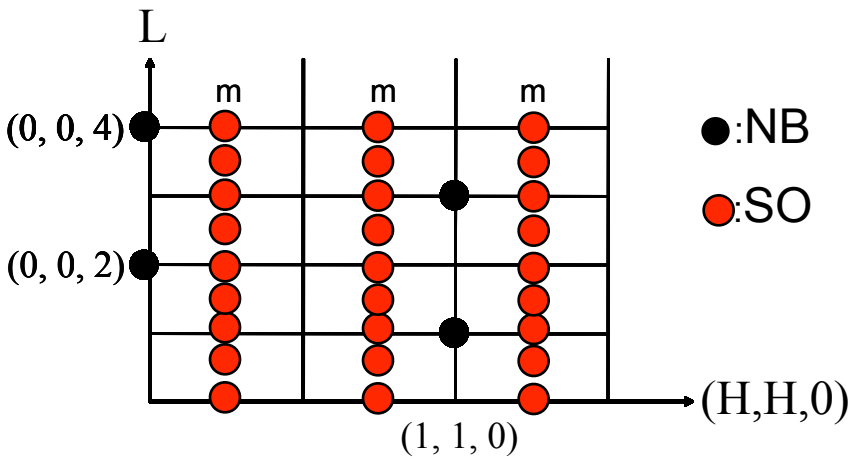

Spin structure of Co^{2+}

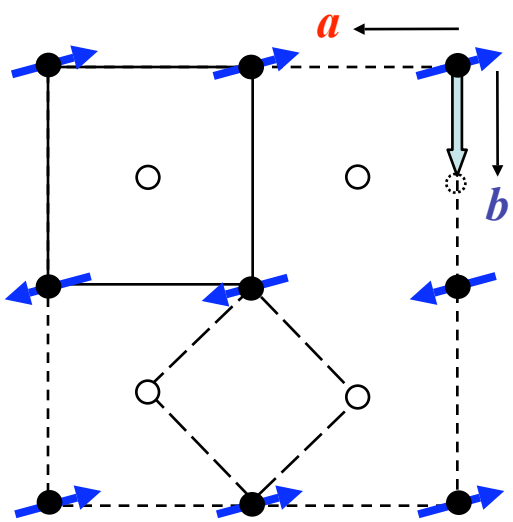

Magnetic unit cell has dimensions **$4a \times 4a \times 2c$** ⟷ Magnetic unit cell has dimensions **$2a \times a \times 2c$**

In-plane correlation lengths for L=half-integer and integer are **93(8) Å, 74(4) Å**, respectively. ⟷ These of correlation lengths are (**195(4) Å, 98(8) Å**).

We concluded that the new magnetic peaks comes from the **Co^{3+} spin supper-lattice peaks**

Co^{3+} spin structure model

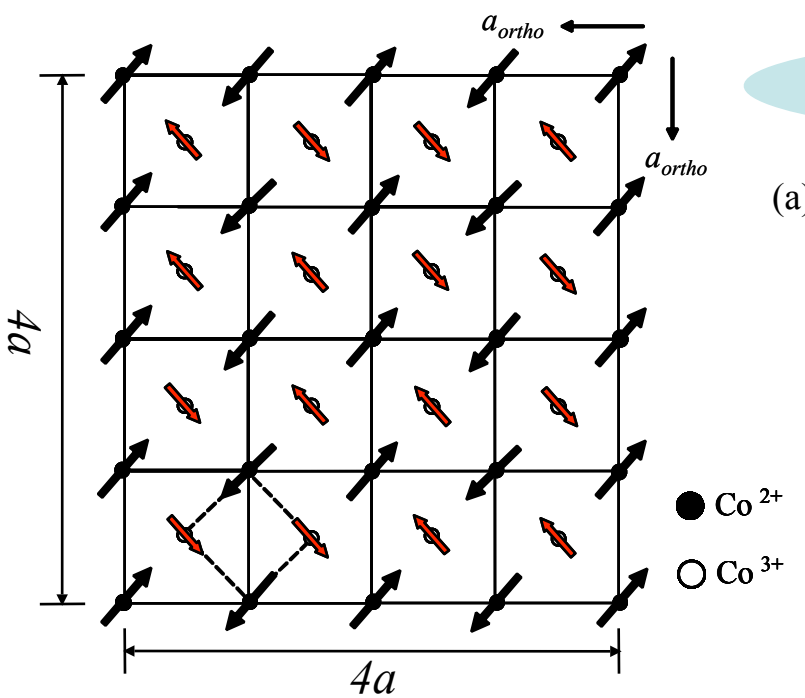

Two types of spin stacking along the *c* axis

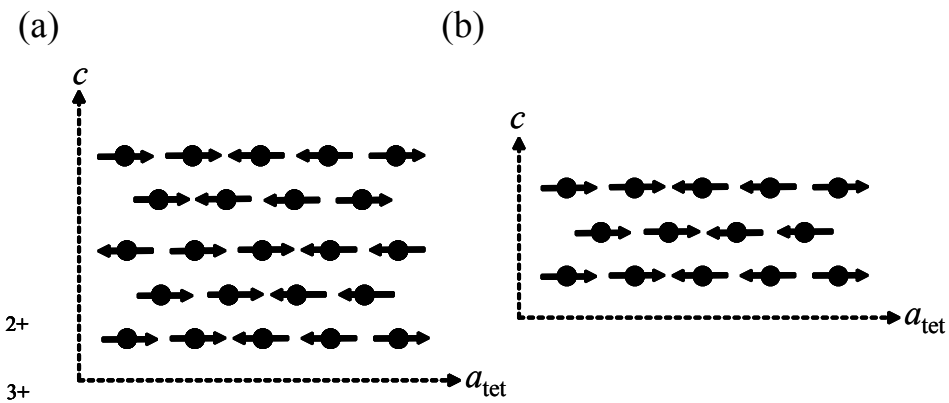

1. magnetic unit cell has dimensions **$4a \times 4a \times 2c$**

   We assumed that the alignment of spin moments is **↑↑↓↓ type** in CoO_2 plane.

2. Two types of **stacking pattern** should be taken into account.
   Two types of spin sackings are considered, and we assumed the magnetic volume fraction to be r=0.315.

Comparison between the calculated and observed magnetic scatterings

peak position	I_{cal}	I_{obs}	$r \cdot I_{cal}$	$(0.5-r) \cdot I_{cal}$
(0.75, 0.75, 0.5)	67.7	22.8	20.3	
(1.25, 1.25, 0.5)	46.0	10.3	13.8	
(0.75, 0.75, 1)	66.1	13.1		15.4
(1.75, 1.75, 1)	42.9	9.3		5.0
(0.75, 0.75, 1.5)	63.0	15.5	18.8	
(1.25, 1.25, 1.5)	42.9	9.9	12.8	
(0.75, 0.75, 2)	59.3	9.0		11.3
(1.25, 1.25, 2)	26.2	4.9		7.7

μ_{Co}^{3+}=3.64(23)μ_B, Φ_s=90°, r (type- I)=0.315

Φs: angle between the spins and the (h,h,0) axis.

- magnetic moment μ_{Co3+}=3.64(23)μ_B

→ **Co^{3+}(HS) is realized** in x=0.5 system.

Hole-doping dependence of charge ordering

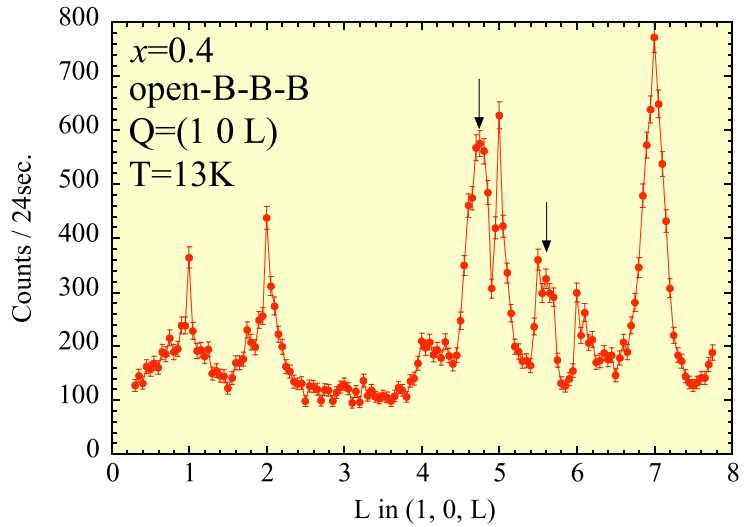

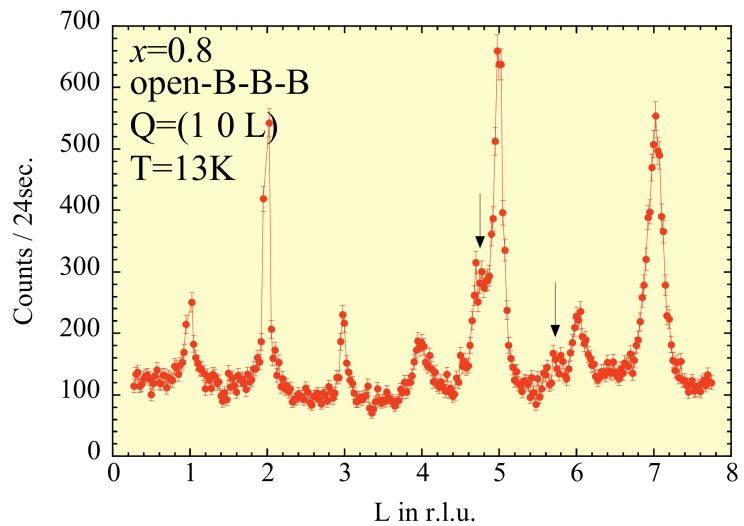

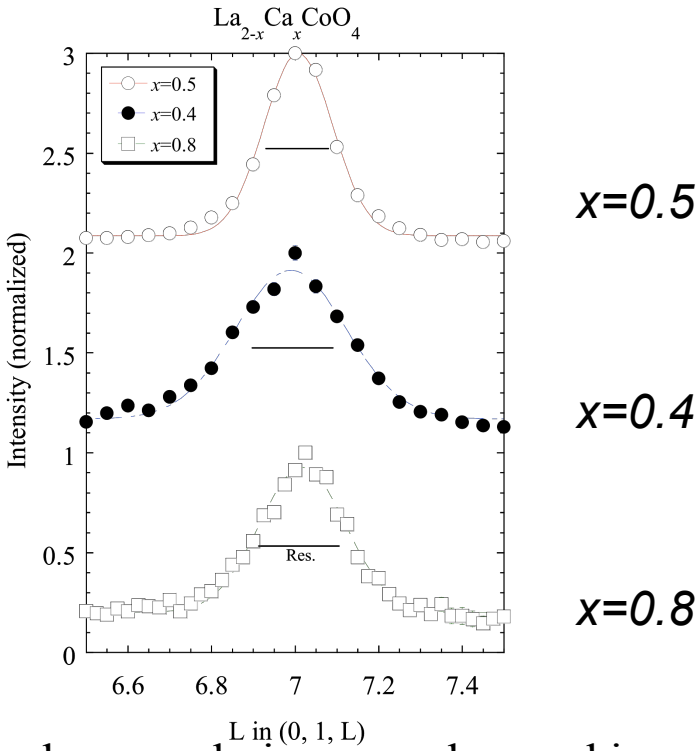

・The charge orderings are observed in **a wide hole doping range**

Robust checkerboard-type charge order

Hole-doping dependence of magnetic ordering

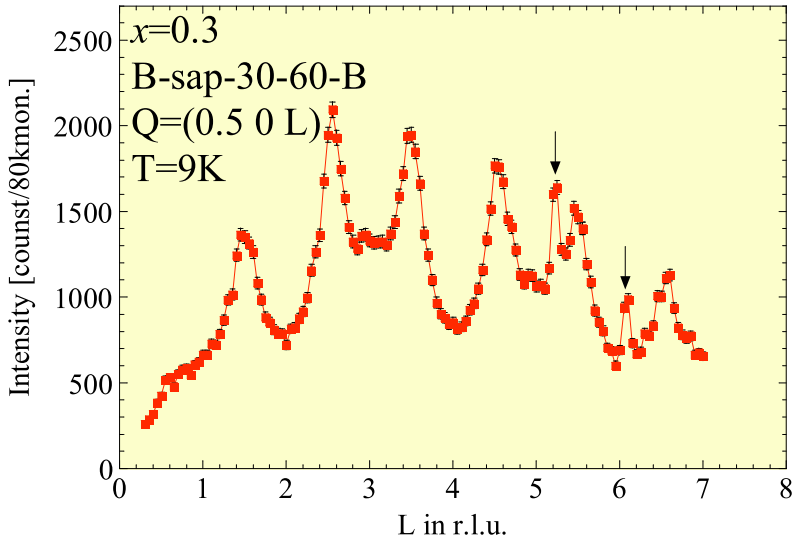

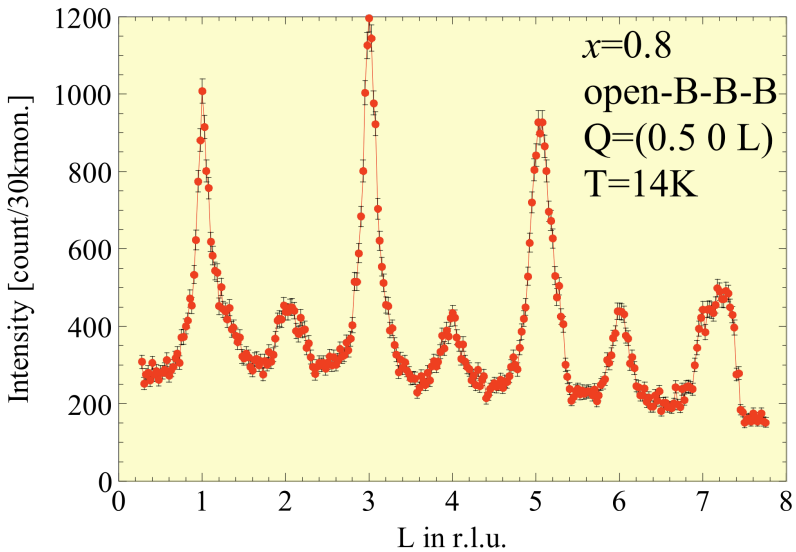

Lower doping region (x<0.5)

Type-I (L=half-integer) reflection arises below x=0.5 together with the **broad diffuse scattering**

Higher doping region (x>0.5)

Type-Ⅱ (L=integer) reflections are observed with a **flat background** in the high doping range of x>0.5.

Dramatically changed by Ca concentration

Magnetic correlation lengths in $La_{2-x}Ca_xCoO_4$

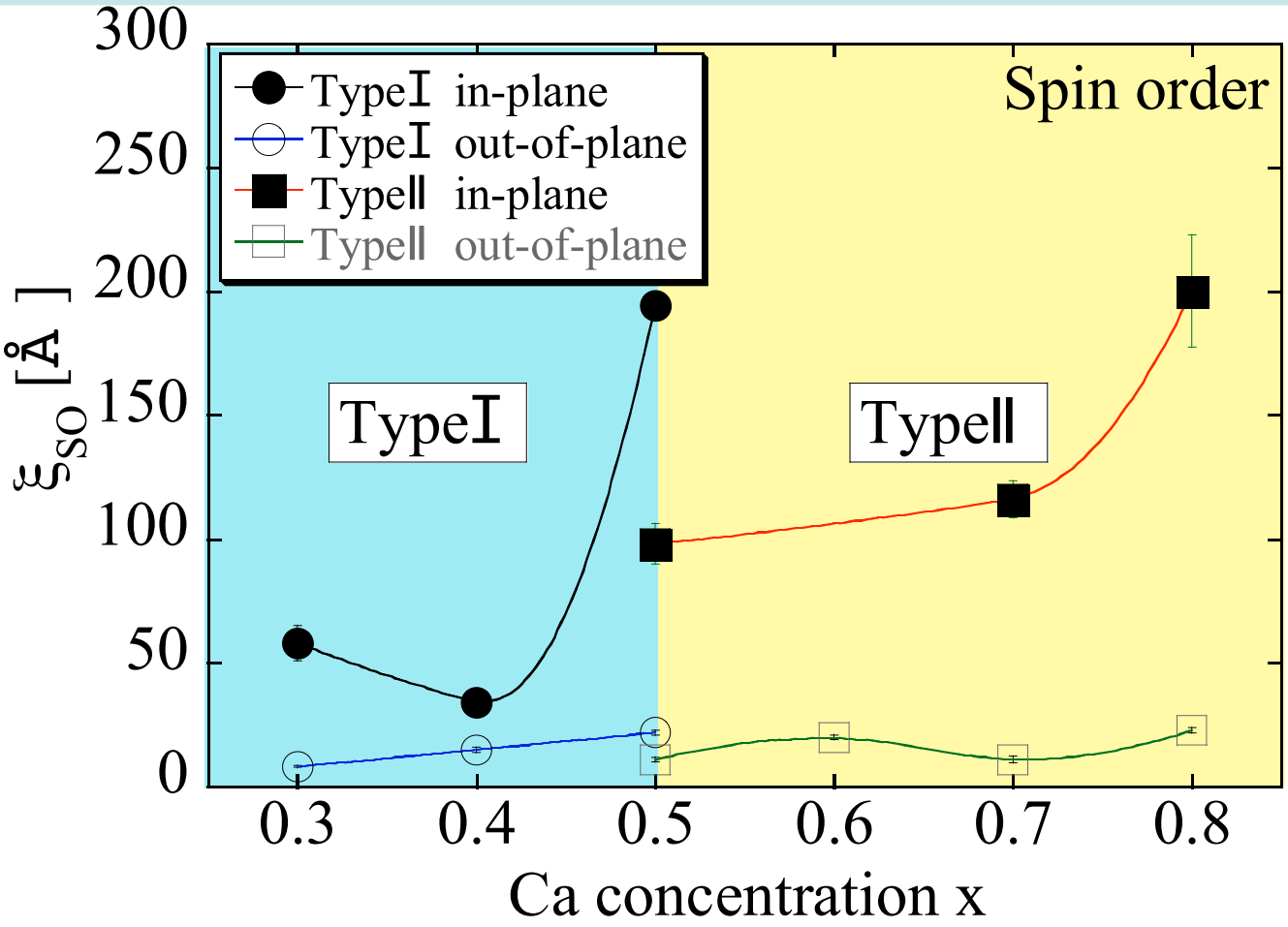

Magnetic domains vs. Ca concentrations

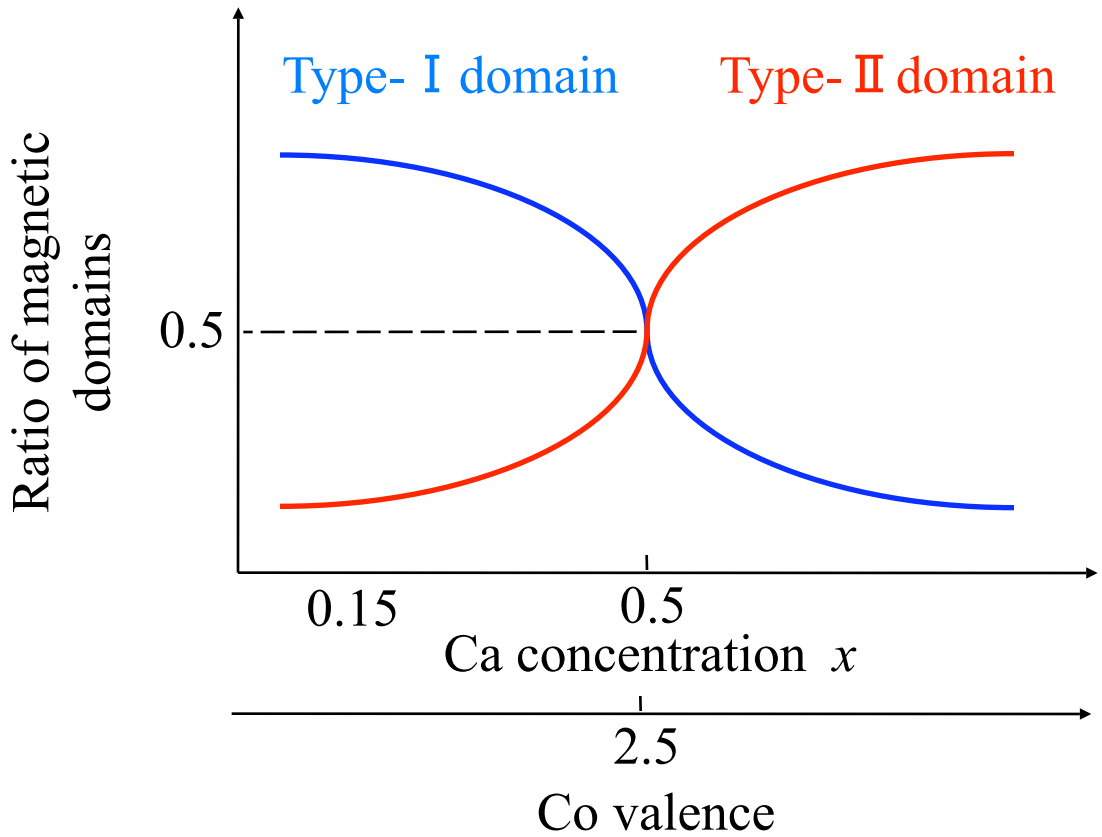

Why type-I and type-II spin domains are clearly separated at Ca-concentration x=0.5?

What is essential for magnetic domains in this system? Ca-concentration or Co-valence

The **excess oxygen** system **$La_{1.85}Ca_{0.15}CoO_{4.17}$**, of which cobalt valence is about **$Co^{2.5+}$, was examined.**

⇨ Only type-I stacking domain peaks were observed in $La_{1.85}Ca_{0.15}CoO_{4.17}$.

The Ca concentration is essential for the magnetic domains.

Hole-doping dependence of Co^{3+} spin magnetic ordering

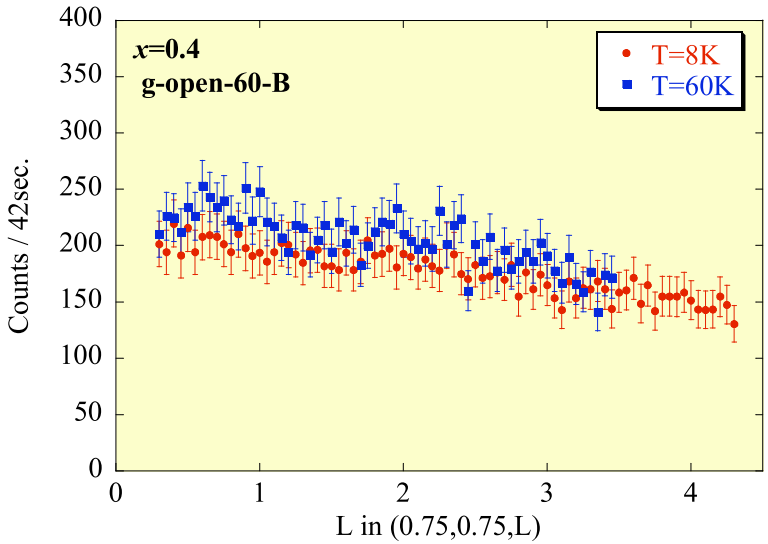

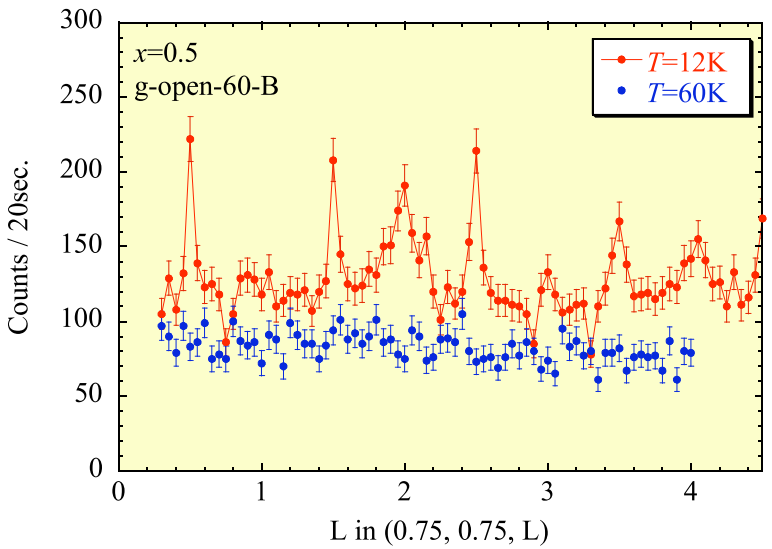

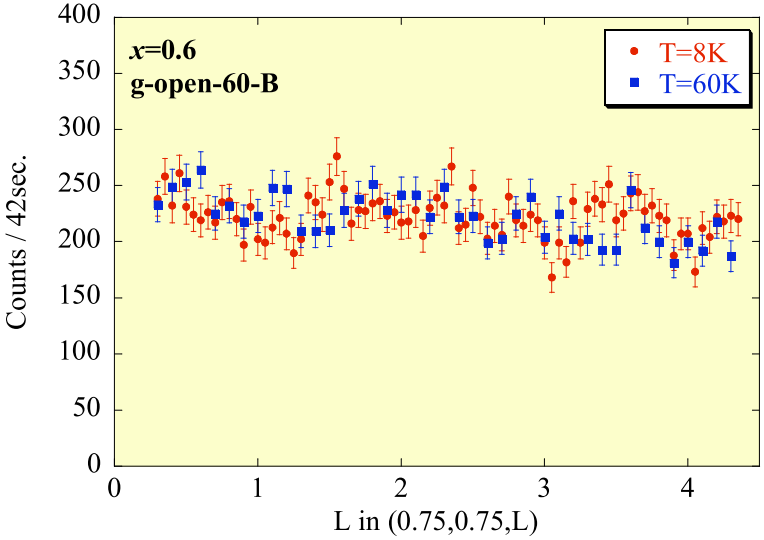

Magnetic ordering of Co^{3+} spin was only observed at ***x*=0.5**

Summary - charge and magnetic structure at x=0.5 -

- **Long rang charge ordering peaks** were observed in Ca system, which can be explained by the **A site** ions.

- Magnetic structure of Co^{2+} spin has been determined .

- The magnitude μ of the Co^{2+} moment was 2.86(19)μ_B to be **Co^{2}+(HS)** .

- Magnetic structure of Co^{3+} spins has been determined at **q=(¼, ¼, ½ or (1)).**

- The magnitude μ of the **Co^{3+}** moment was 3.64(23) μ_B to be **HS state**.

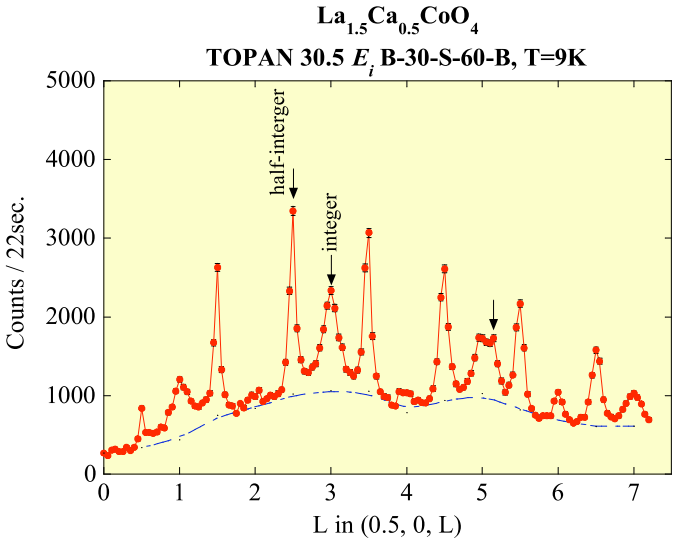

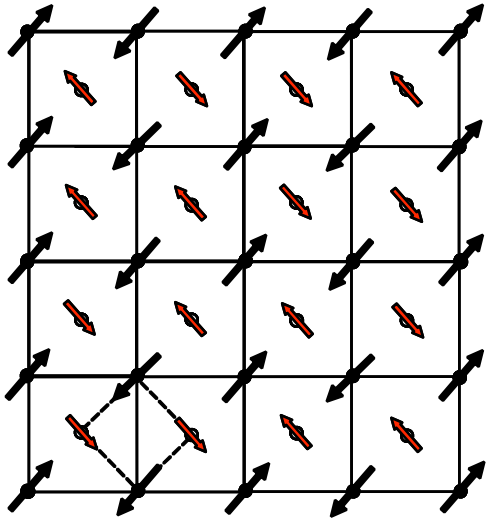

Summary -hole-doping dependence-

・We observed robust commensurate **charge ordered** peaks in **a wide doping range**.

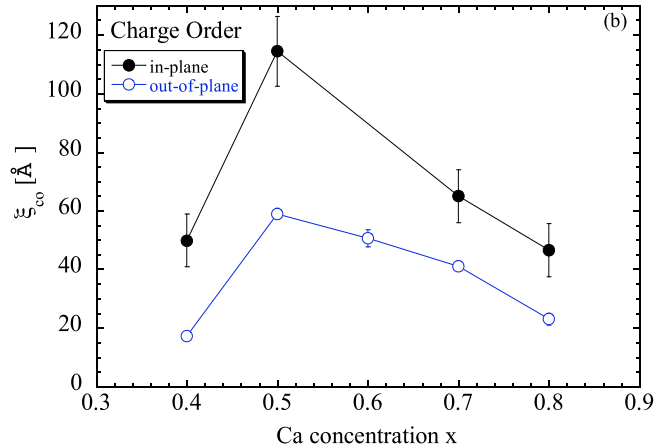

・ **Magnetic scattering** pattern are drastically **changed at *x*=0.5**.

・From magnetic peaks for $La_{1.85}Ca_{0.15}CoO_{4.17}$, **magnetic domains are changed by Ca substitutions.**

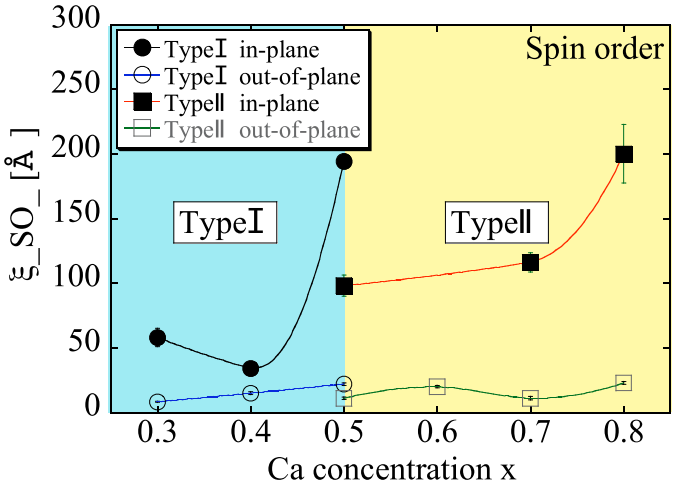

§3 Ultrasound measurement in $La_{2-x}Ca_xCoO_4$ ($0.4<x<0.7$)

Pulse echo method

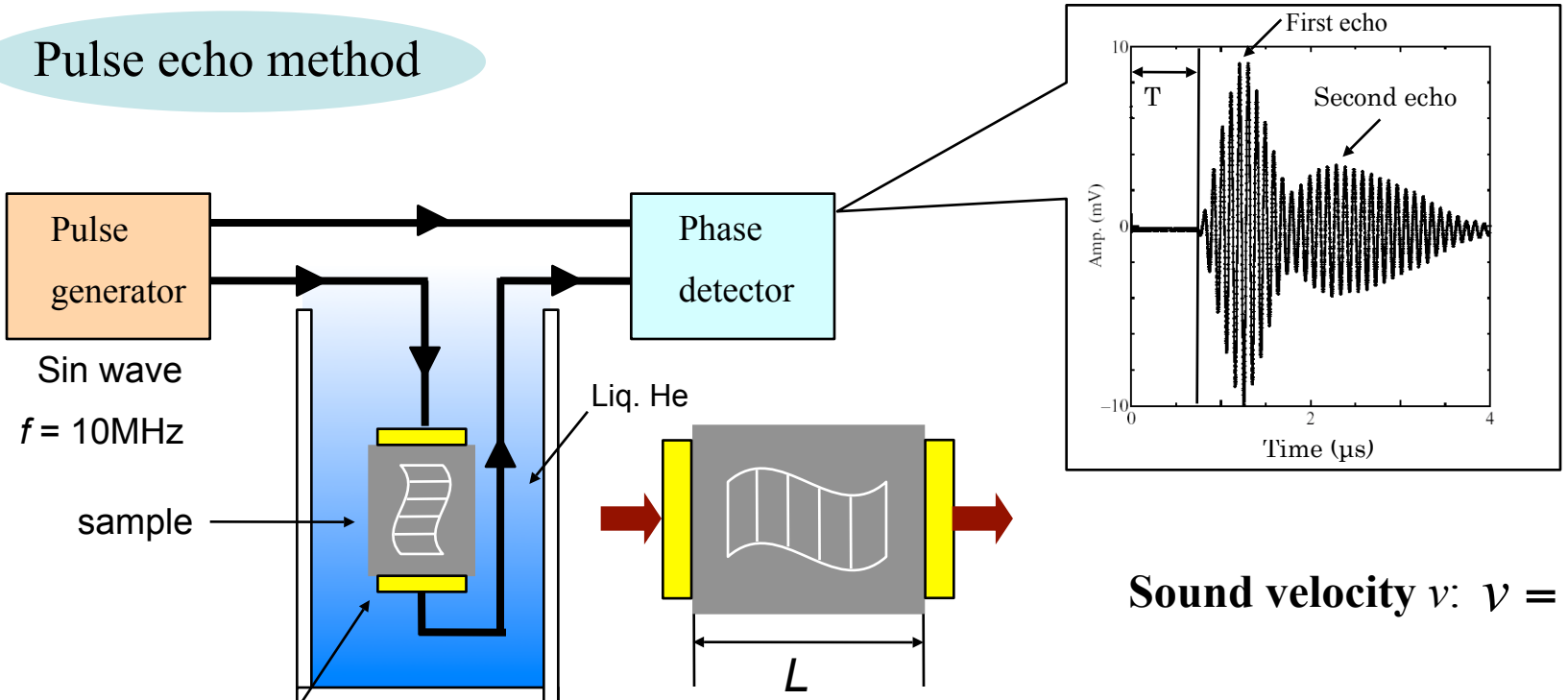

Transducer ($LiNbO_3$) : Convert electrical signal into mechanical one.

Sound velocity v: $v = \dfrac{L}{T}$

Elastic constant C_{eff}: $C_{eff} = \rho v^2$

ρ : density of the solids

Sound velocities in $La_{1.5}Ca_{0.5}CoO_4$

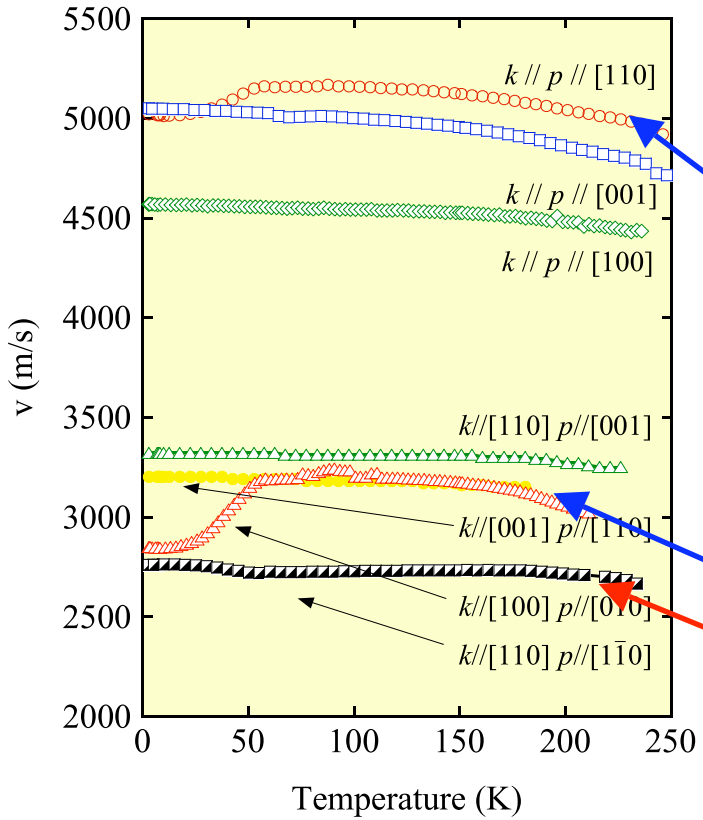

We observed anomalies near T_N(~50K)

Effective elastic constants for propagating ***k*** and polarization ***p***

k //	p //	C_{eff}
[110]	[110]	$\frac{C_{11}-C_{12}+2C_{66}}{2}$
[001]	[001]	C_{33}
[100]	[100]	C_{11}
[110]	[001]	C_{44}
[001]	[110]	C_{13}
[100]	[010]	C_{66}
[110]	[1$\bar{1}$0]	$\frac{C_{11}-C_{12}}{2}$

We indexed ***k*** and ***p*** vector by a CO unit cell

Softening: $\frac{C_{11}-C_{12}+2C_{66}}{2}, C_{66}$

Hardening: $\frac{C_{11}-C_{12}}{2}$

Ca dependence of sound velocity for C_{66}

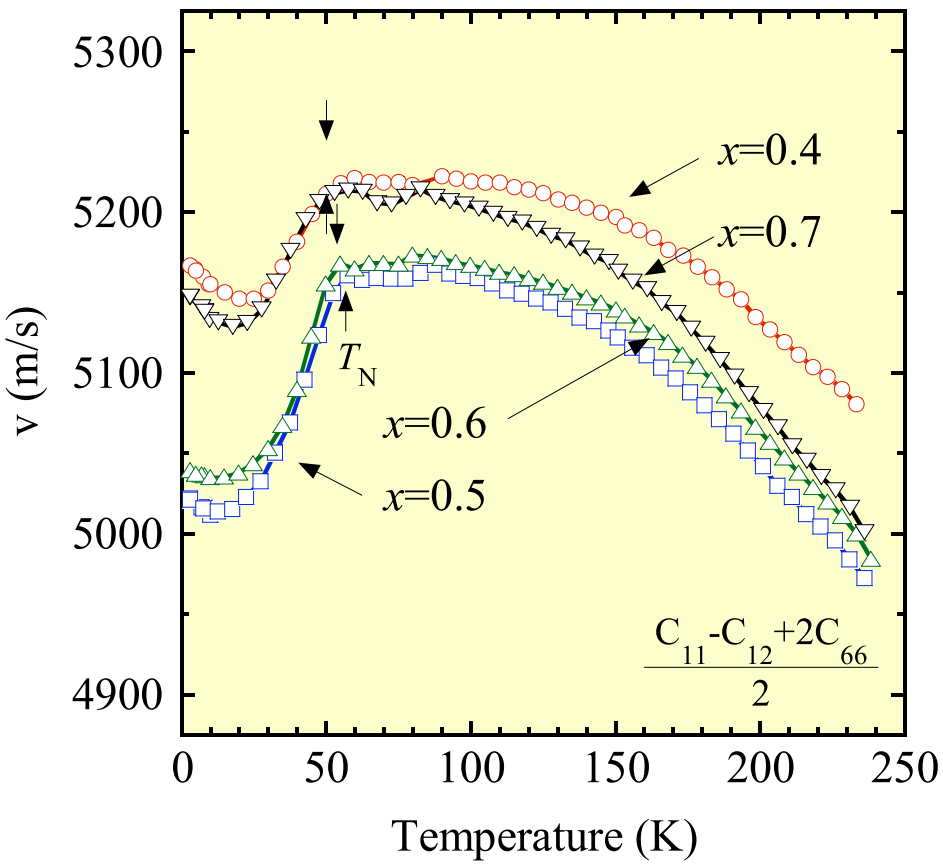

(1) The anomalous softenings were observed **in the whole doping range.**

(2) Starting temperature of softening agree well with T_N

Elastic constant C_{66} and attenuation coefficient α_{c66}

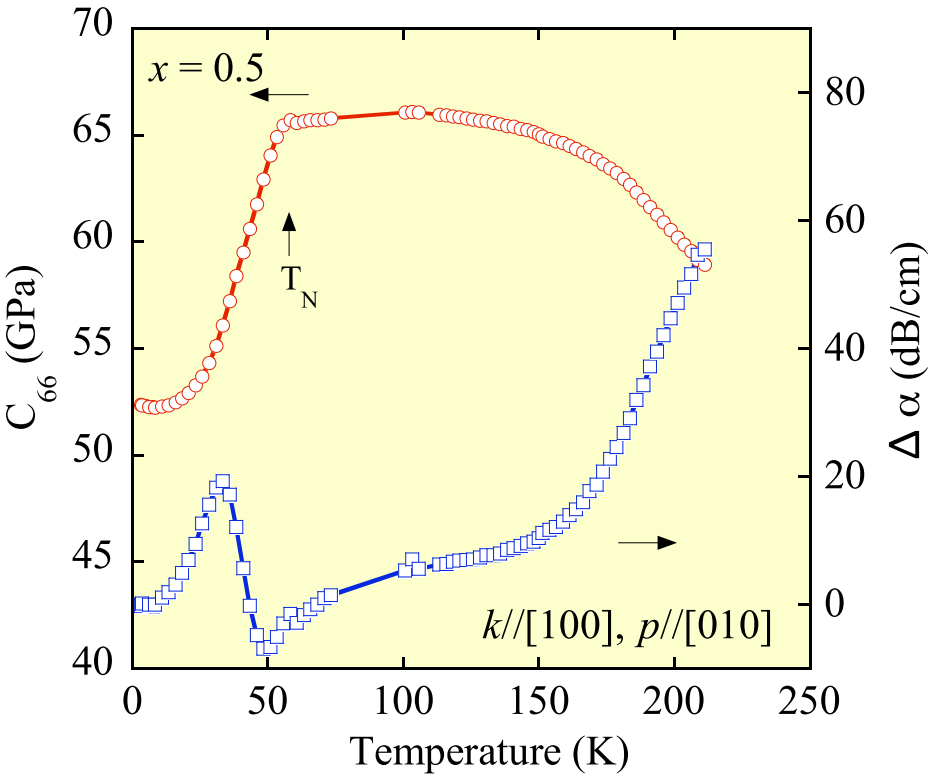

1. The large softening (20%) below T_N shows the stepwise behavior.

2. The temperature dependence of α below T_N shows strange behavior.

Elastic constant C_{66} and attenuation coefficient α_{c66}

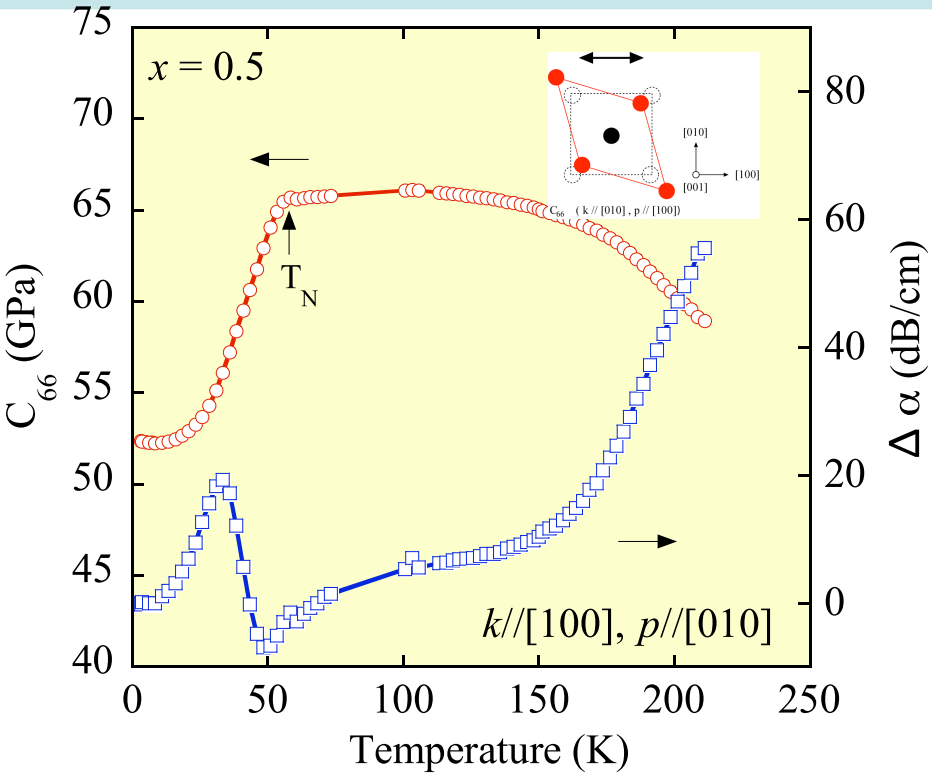

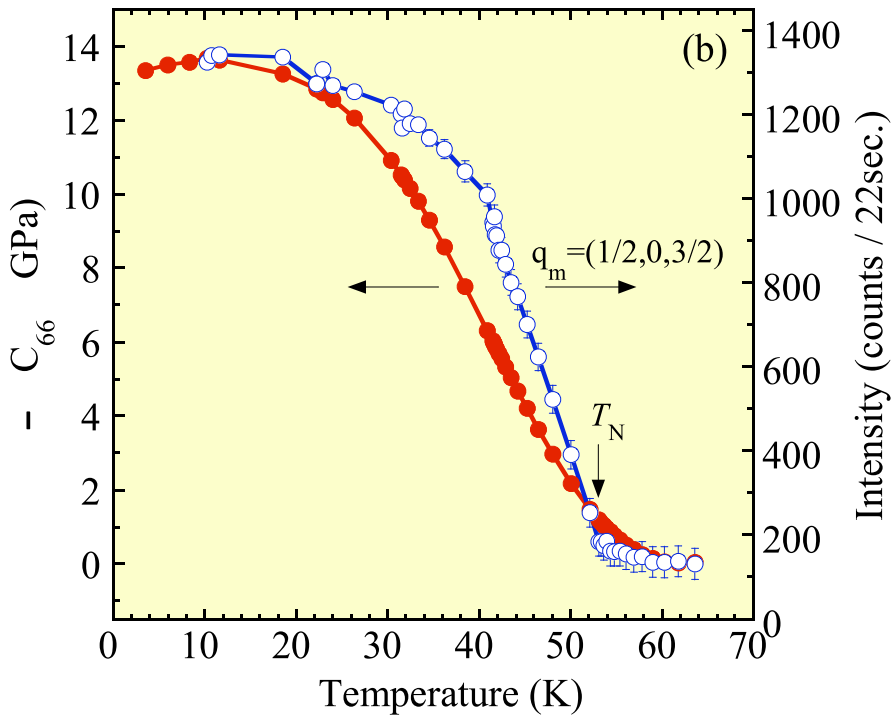

Temperature dependence of -⊿C_{66} is similar to the that of magnetic scattering intensity.

The strain relevant to C_{66} is **strongly correlated with this magnetic ordering (q=(1/2, 0, 3/2))**

Construction of Landau free energy for $La_{2-x}Ca_xCoO_4$

Order parameter

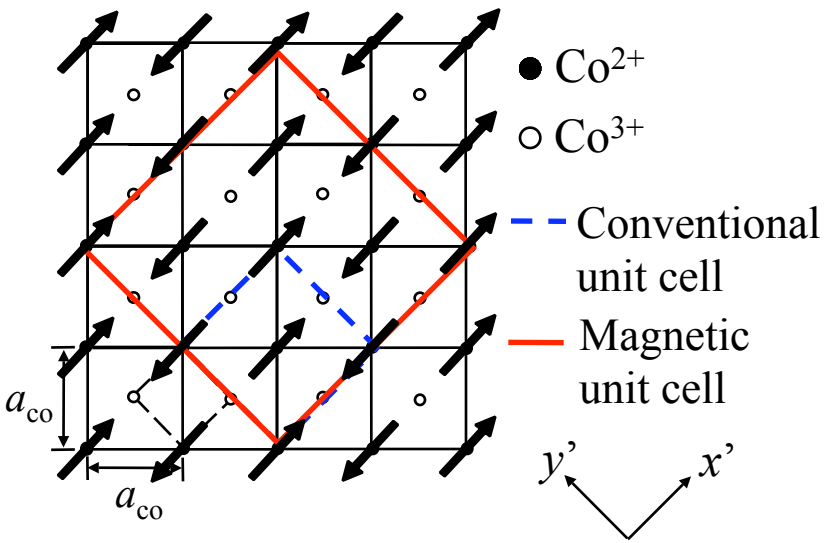

The strain relevant to C_{66} is [110]

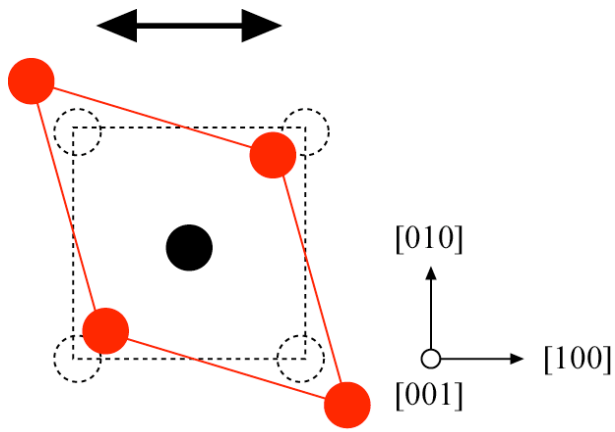

C_{66} (k // [010] , p // [100])

"transverse-like" spin modulation along the y' ([110]) direction ($\boldsymbol{k} \perp \boldsymbol{s}$) as order parameter

$$Q_1 = Q_{10} \exp(i\pi \frac{y'}{\sqrt{2}a_{co}})$$

$$Q_2 = Q_{20} \exp(i\pi \frac{x'}{\sqrt{2}a_{co}})$$

The observed step wise behavior of C_{66}

Improper coupling

$$gQ^2u$$

g: coupling constant

Q: Order parameter

u: elastic strain

Construction of Landau free energy for $La_{2-x}Ca_xCoO_4$

Order parameter

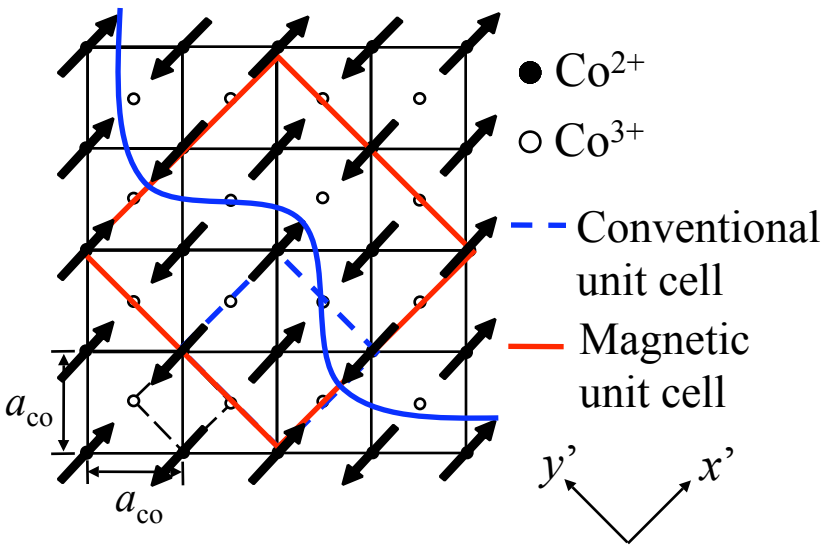

The strain relevant to C_{66} is [110]

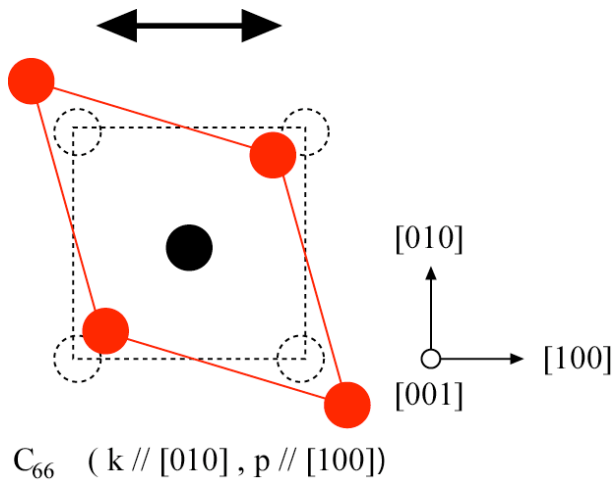

"transverse-like" spin modulation along the y' ([110]) direction ($\boldsymbol{k} \perp \boldsymbol{s}$) as order parameter

$$Q_1 = Q_{10} \exp(i\pi \frac{y'}{\sqrt{2}a_{co}})$$

$$Q_2 = Q_{20} \exp(i\pi \frac{x'}{\sqrt{2}a_{co}})$$

The observed step wise behavior of C_{66}

Improper coupling

$$gQ^2u$$

g: coupling constant

Q: Order parameter

u: elastic strain

Construction of Landau free energy for $La_{2-x}Ca_xCoO_4$

Order parameter

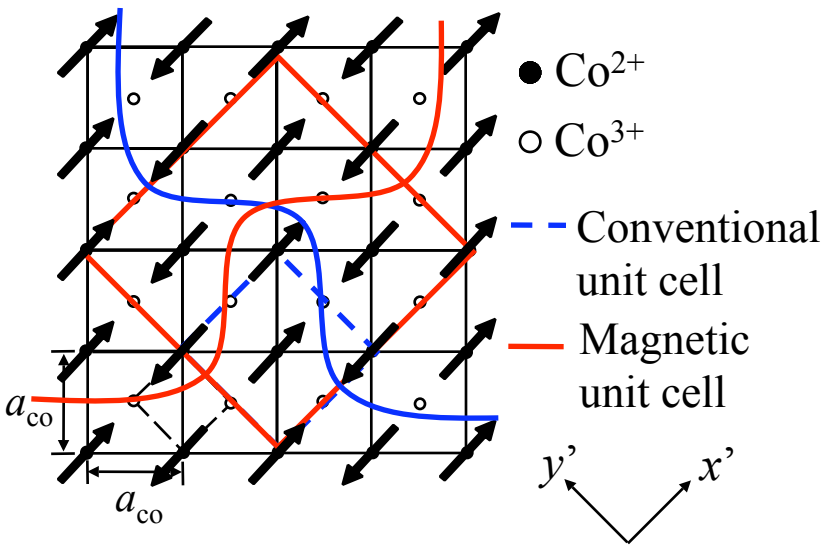

The strain relevant to C_{66} is [110]

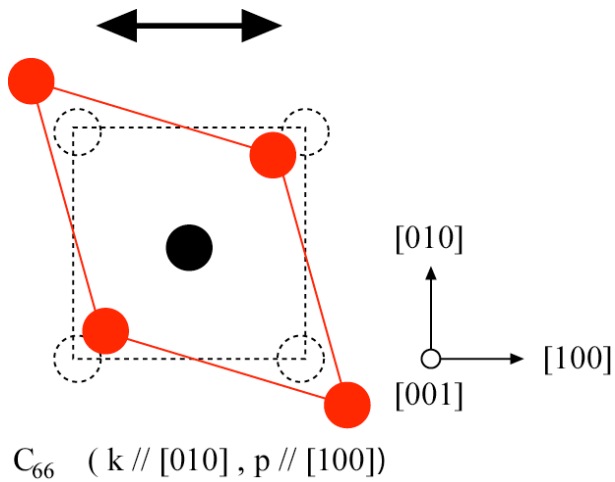

"transverse-like" spin modulation along the y' ([110]) direction ($\boldsymbol{k} \perp \boldsymbol{s}$) as order parameter

$$Q_1 = Q_{10} \exp(i\pi \frac{y'}{\sqrt{2}a_{co}})$$

$$Q_2 = Q_{20} \exp(i\pi \frac{x'}{\sqrt{2}a_{co}})$$

The observed step wise behavior of C_{66}

Improper coupling

$$gQ^2u$$

g: coupling constant

Q: Order parameter

u: elastic strain

Landau free energy for $La_{2-x}Ca_xCoO_4$

The free energy *F*

up to the fourth order of the order parameter was expressed as

$$F = F_0 + \frac{\alpha}{2}(Q_{10}^2 + Q_{20}^2) + \frac{\beta}{4}(Q_{10}^4 + Q_{20}^4) + \frac{\gamma}{2}(Q_{10}^2 Q_{20}^2)$$

$$+ \zeta_1 u_1 (Q_{10} Q_{20}) + \frac{1}{2}\zeta_2 u_2 (Q_{10}^2 - Q_{20}^2)$$

$$+ \frac{1}{2} C_1^{(para)} u_1^2 + \frac{1}{2} C_2^{(para)} u_2^2$$

Landau free energy for $La_{2-x}Ca_xCoO_4$

The free energy *F*

up to the fourth order of the order parameter was expressed as

$$F = F_0 + \frac{\alpha}{2}(Q_{10}^2 + Q_{20}^2) + \frac{\beta}{4}(Q_{10}^4 + Q_{20}^4) + \frac{\gamma}{2}(Q_{10}^2 Q_{20}^2)$$

$$+ \zeta_1 u_1 (Q_{10} Q_{20}) + \frac{1}{2}\zeta_2 u_2 (Q_{10}^2 - Q_{20}^2)$$

$$+ \frac{1}{2} C_1^{(para)} u_1^2 + \frac{1}{2} C_2^{(para)} u_2^2$$

Landau free energy for $La_{2-x}Ca_xCoO_4$

The free energy *F*

up to the fourth order of the order parameter was expressed as

$$F = F_0 + \frac{\alpha}{2}(Q_{10}^2 + Q_{20}^2) + \frac{\beta}{4}(Q_{10}^4 + Q_{20}^4) + \frac{\gamma}{2}(Q_{10}^2 Q_{20}^2)$$

$$+ \zeta_1 u_1 (Q_{10} Q_{20}) + \frac{1}{2}\zeta_2 u_2 (Q_{10}^2 - Q_{20}^2)$$

$$+ \frac{1}{2} C_1^{(para)} u_1^2 + \frac{1}{2} C_2^{(para)} u_2^2$$

Improper coupling terms of $(C_{11}-C_{12})/2$ and C_{66}

u_1, u_2: strains corresponds to $(C_{11}-C_{12})/2$ and C_{66}

Landau free energy for $La_{2-x}Ca_xCoO_4$

The free energy *F*

up to the fourth order of the order parameter was expressed as

$$F = F_0 + \frac{\alpha}{2}(Q_{10}^2 + Q_{20}^2) + \frac{\beta}{4}(Q_{10}^4 + Q_{20}^4) + \frac{\gamma}{2}(Q_{10}^2 Q_{20}^2)$$

$$+ \zeta_1 u_1 (Q_{10} Q_{20}) + \frac{1}{2}\zeta_2 u_2 (Q_{10}^2 - Q_{20}^2)$$

$$+ \frac{1}{2} C_1^{(para)} u_1^2 + \frac{1}{2} C_2^{(para)} u_2^2$$

Improper coupling terms of $(C_{11}-C_{12})/2$ and C_{66}

u_1, u_2: strains corresponds to $(C_{11}-C_{12})/2$ and C_{66}

Landau free energy for $La_{2-x}Ca_xCoO_4$

The free energy *F*

up to the fourth order of the order parameter was expressed as

$$F = F_0 + \frac{\alpha}{2}(Q_{10}^2 + Q_{20}^2) + \frac{\beta}{4}(Q_{10}^4 + Q_{20}^4) + \frac{\gamma}{2}(Q_{10}^2 Q_{20}^2)$$

$$+ \zeta_1 u_1 (Q_{10} Q_{20}) + \frac{1}{2}\zeta_2 u_2 (Q_{10}^2 - Q_{20}^2)$$

$$+ \frac{1}{2} C_1^{(para)} u_1^2 + \frac{1}{2} C_2^{(para)} u_2^2$$

Improper coupling terms of $(C_{11}-C_{12})/2$ and C_{66}

u_1, u_2: strains corresponds to $(C_{11}-C_{12})/2$ and C_{66}

Elastic energies of $(C_{11}-C_{12})/2$ and C_{66}

C_1, C_2: elastic constants corresponds to $(C_{11}-C_{12})/2$ and C_{66}

The minimization of free energy

Three sets of the stable solution are obtained

Case(Ⅰ) $Q_{10} = Q_{20} = 0$ **(paramagnetic phase)**

Case(Ⅱ) $Q_{10} \neq 0$, $Q_{20} = 0$ **or** $Q_{10} = 0$, $Q_{20} \neq 0$

"transverse-like" spin modulation along the *y*' or *x*' direction

Case(Ⅲ) $Q_{10} = Q_{20} \neq 0$ **or** $Q_{10} = -Q_{20} \neq 0$

The modulation along the [010] or [100] direction

As compared with the spin configuration, **Case(Ⅱ)** is realized.

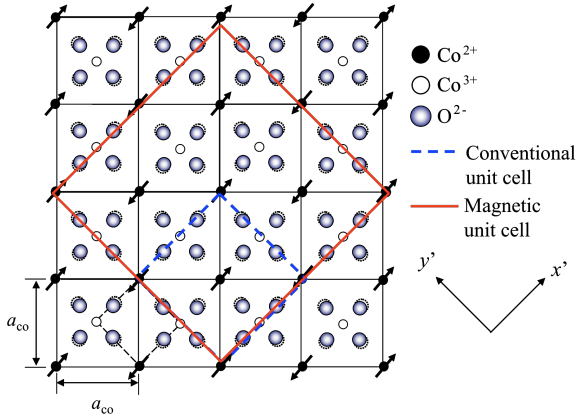

Anomalies of C_{66}

In case(Ⅱ), the elastic constant C_{66} was obtained as

$$C_{66} = C_2^{(para)} \qquad (T > T_N)$$

$$C_{66} = C_2^{(para)} - \frac{\zeta_2^2}{2\beta} \qquad (T < T_N)$$

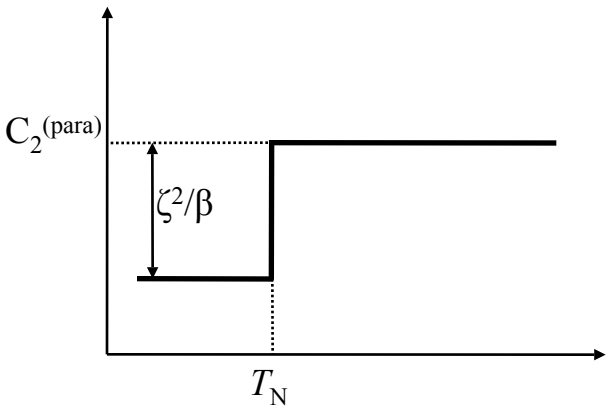

C_{66} is constant in the paramagnetic phase, and decreases stepwise in the ordered phase.

The **stepwise softening of C_{66} related with magnetic ordering can be explained** based on Landau theory.

The origin of order parameter ①

Magnetic striction (?)

1. Magnetic ordering may lead to elastic anomalies which is proportional to the square of the magnetic moment.

2. The softening starts around the magnetic ordering temperature.

However

1. Magnetic striction is not large enough to explain the observed giant softening.
2. Why only the C_{66} mode appears in the magnetic striction?
3. Improper coupling has a hidden order parameter, suggesting **spin modulation is unsuitable.**

The origin of order parameter ②

Orbital ordering (?)

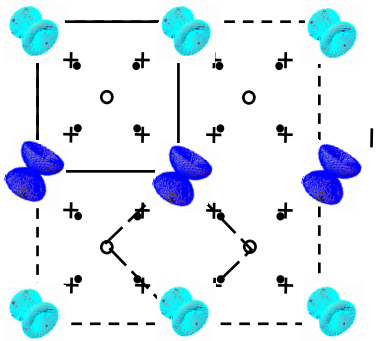

1. The **orbital ordering modulation** along [110] and [-110] can be also regarded as **order parameter.**

2. C_{66} belongs to B_{1g} irreducible representation symmetry which correspond to the **JT-mode**.

3. The attenuation coefficient behavior suggests that there is the **presence of the fluctuation** in zig-zag orbital ordering.

Summary on ultrasound velocity in $(La,Ca)_2CoO_4$

- A **giant softening of C_{66}** was observed below T_N in all concentrations.

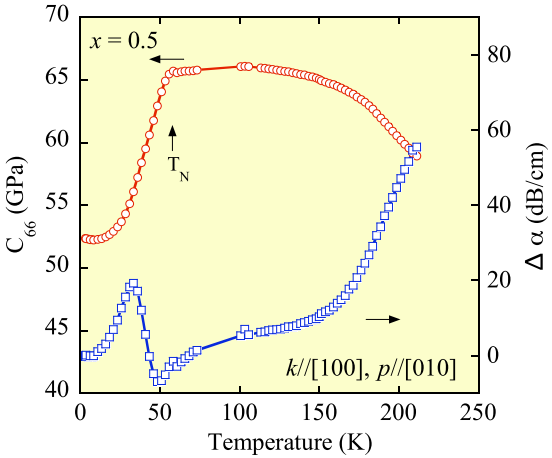

- The novel softening of C_{66} was discussed by Landau theory and this theory explained well the stepwise behavior.

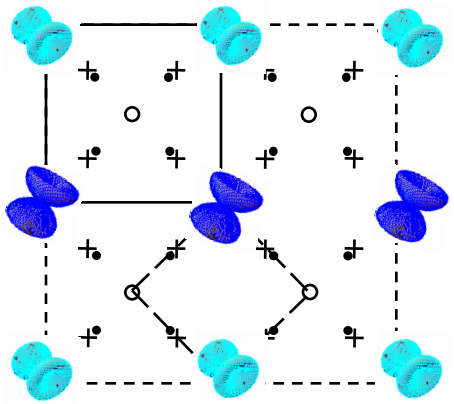

Question

- I would like to ask overall understanding between the C_{66} softening and magnetic structure in $(La,Ca)_2CoO_4$.

Superconductivity in B-doped SiC
-Collaborators-

- Z.-A. Ren, J. Kato, T. Muranaka
- AC susceptibility
  - M. Kriener, Y. Maeno (Kyoto Univ.)

JPSJ Vol.76 No.10 (2007) 103710

Thanks to the editors for choosing this paper as **"Paper of Editors' Choice"**.

Searching for new superconductivity in a wide gap semiconductor with a diamond lattice structure

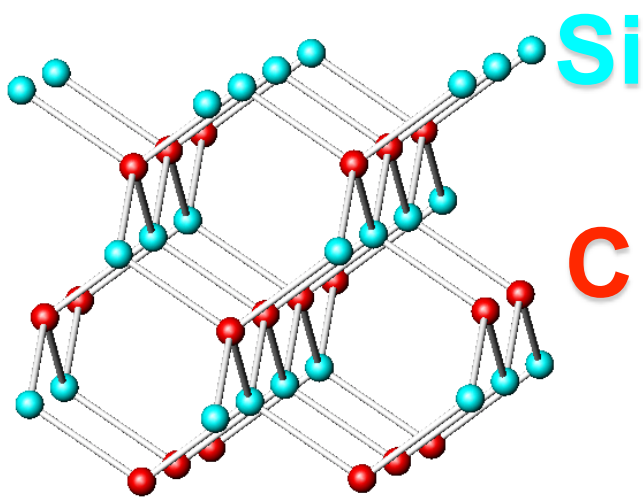

Crystal structure of 3C-SiC

a = 0.436 nm
SG: F-43m
Band Gap: 2.23 eV

- We try to dope B atom for carrier doping.
- But…. many polytypes exist in SiC.
  - β-SiC
    - 3C-SiC (diamond-type structure)
  - α-SiC
    - nH-SiC(2H-SiC, 4H-SiC, 6H-SiC etc.)
    - nR-SiC(15R-SiC, 21R-SiC etc.)

Temperature dependence of resistivity

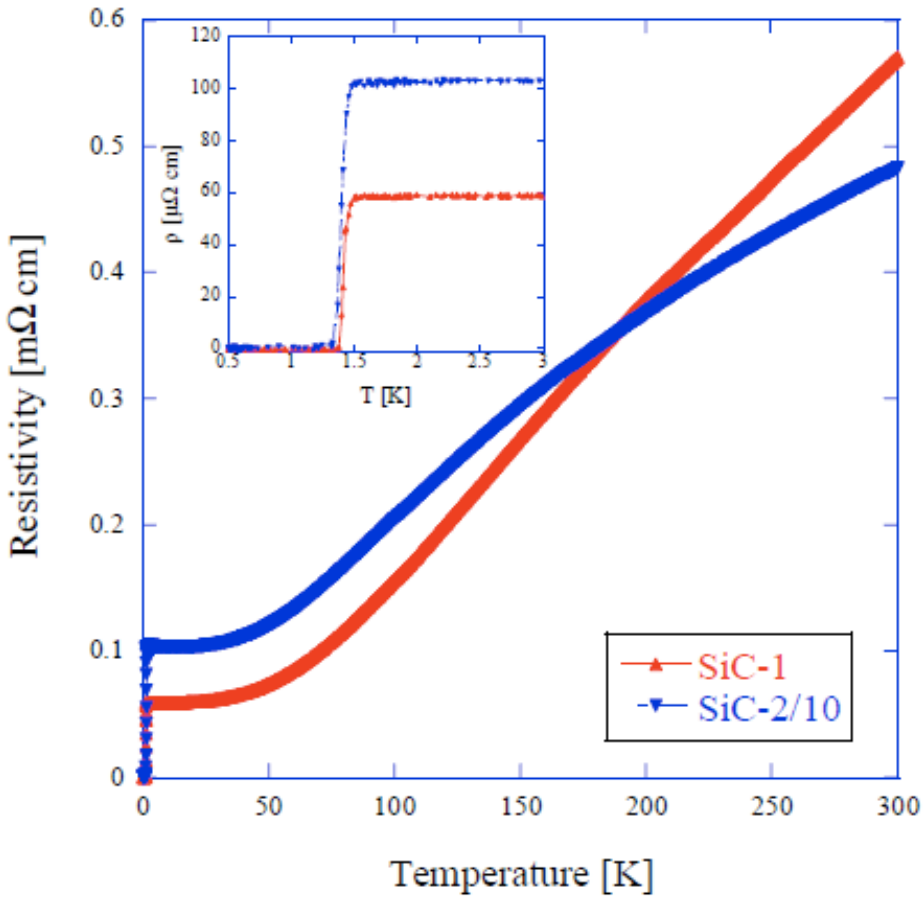

- Superconductivity was observed at T_c=1.4 K

Aoyama-Gakuin University

Temperature dependence of AC susceptibility

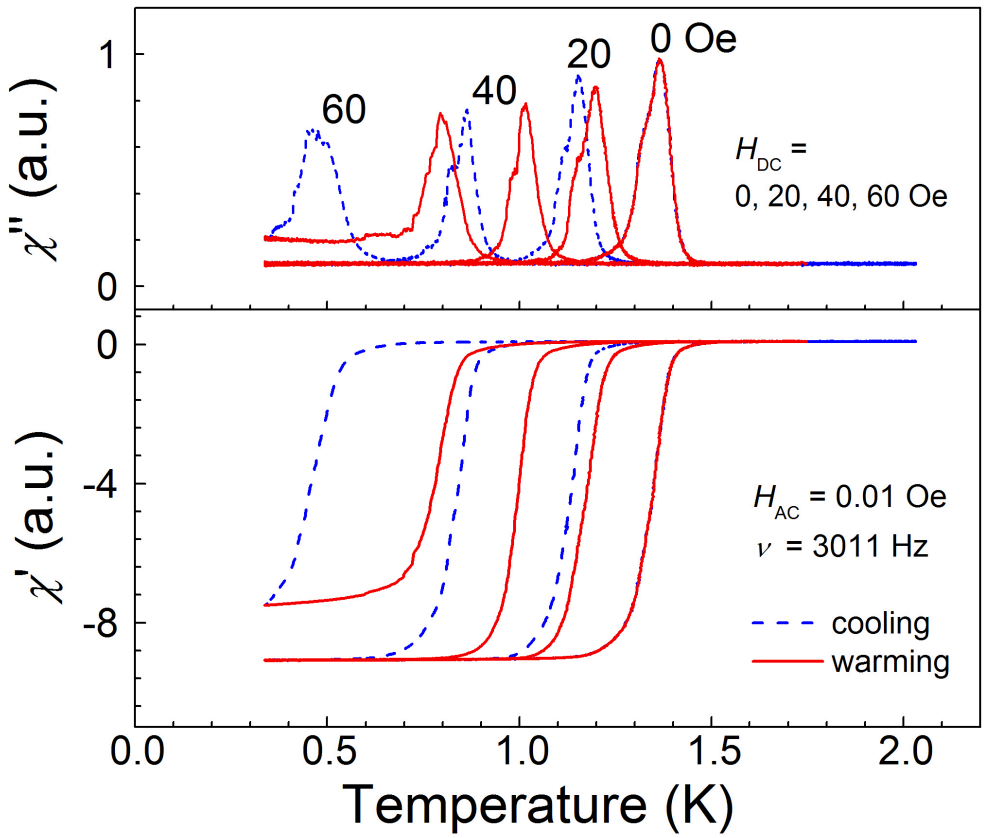

- We observed the in-field hysteresis and the absence of a hysteresis in zero field.
  - Strong evidence for **type-I superconductivity**.

H-T phase diagram from AC susceptibility

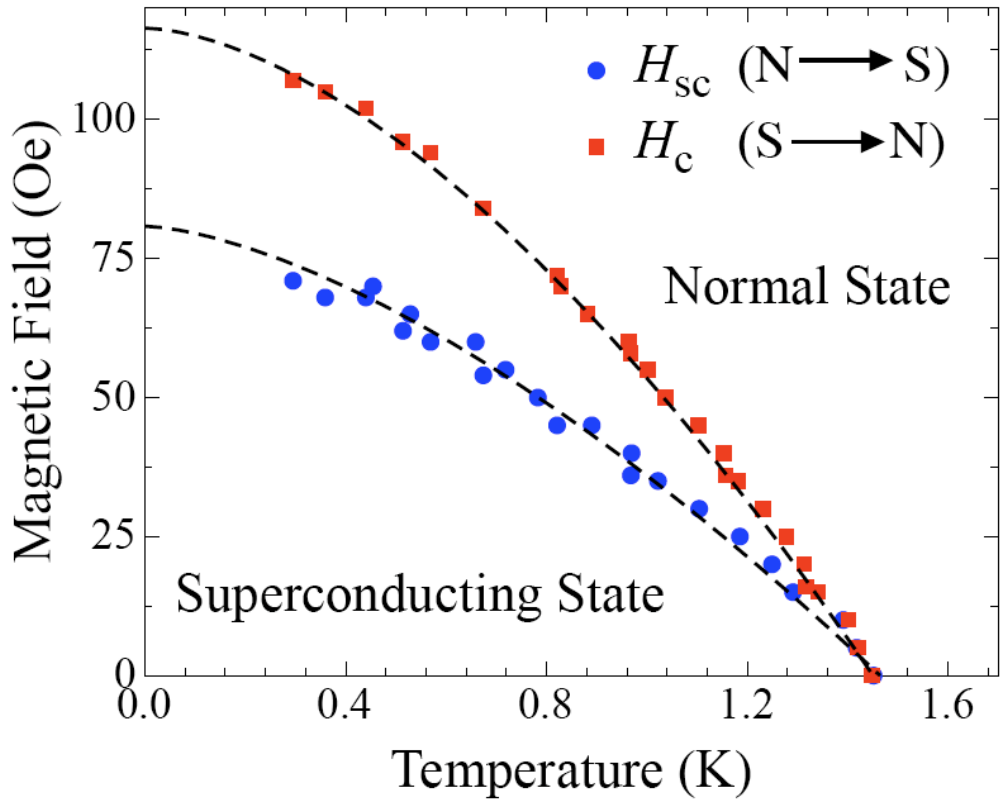

- We determined $H_{sc}(0)$ to be (83±5) Oe
  - GL parameter $\kappa \leq 0.34$ (type-I)

Comparison with literature

	SiC-1	SiC-2	C:B (Sidorov *et al.*)	Si:B (Bustarret *et al.*)
n (cm^{-3})	$1.91 \cdot 10^{21}$	$1.06 \cdot 10^{21}$	$1.80 \cdot 10^{21}$	$2.80 \cdot 10^{21}$
γ (mJ/molK^2)	0.29	0.22	0.113	
β (mJ/molK^4)	0.019	0.017	0.0007	
Θ_D (K)	590	610	1440	
ρ_0 ($\mu\Omega$cm)	60	1030	2500	130
RRR	10	5	0.9	1.23
$T_c(H=0)$ (K)	1.45	1.42	4.5	0.35
$\Delta C/\gamma T_c$	0.96	0.80	0.5	
$\xi(0)$ (nm)	360	330	9	20
$\lambda(0)$ (nm)	130	170	163	
$\kappa_{GL}(0)$	0.36	0.52	18	

- These materials have same crystal structure and carrier density.
- But, only SiC:B is type-I superconductor because of the very long coherence length.

Superconductivity in B-doped SiC

3C-SiC

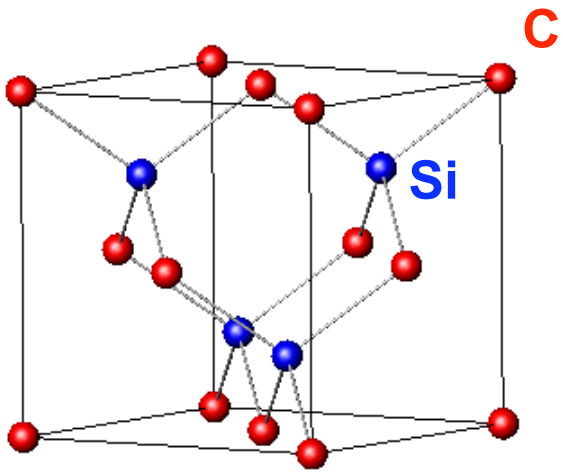

OR

6H-SiC

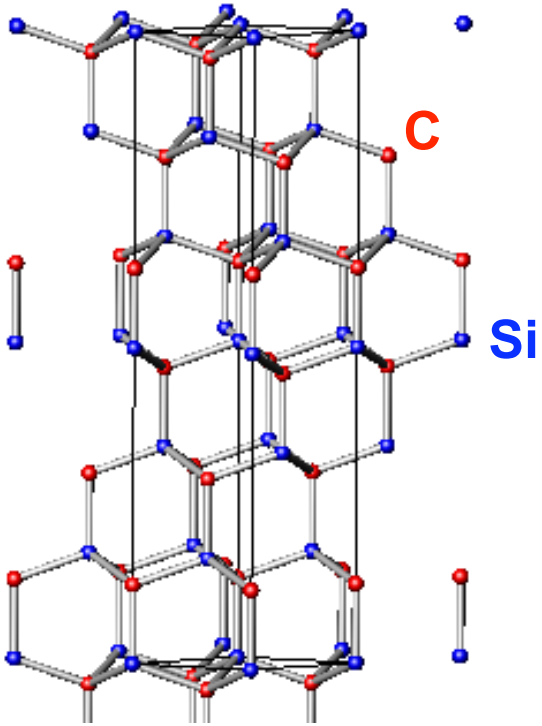

- Stacking of C-layer and Si-layer and its direction are different.
  - 3C-SiC; along <111>
  - 6H-SiC; along <001>

Band dispersion of 3C-SiC & 6H-SiC

3C-SiC

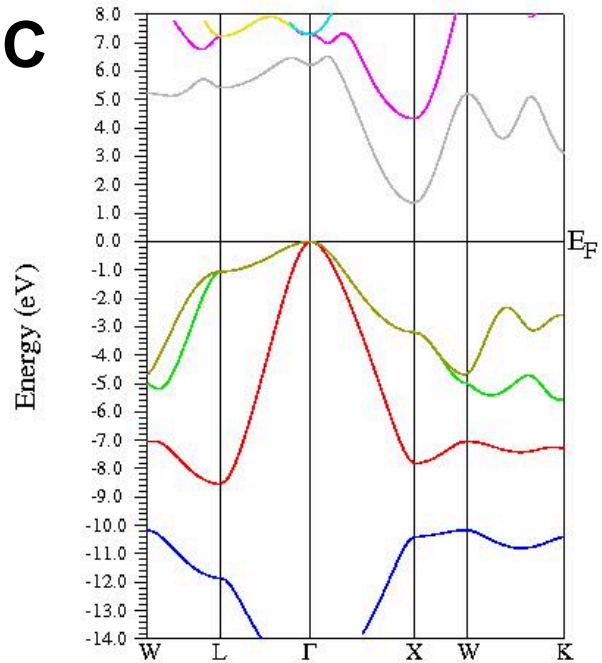

6H-SiC

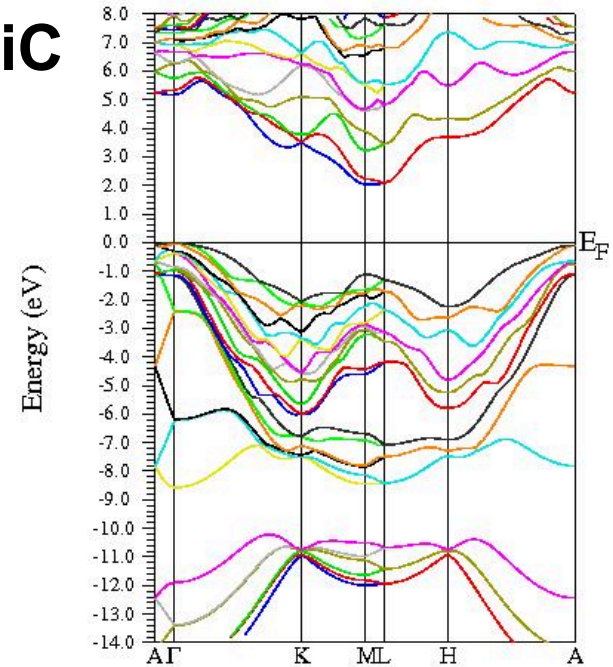

- Indirect gap: ~2eV
- Top of valence bands are located almost E_F in both types.
- Almost same Debye temperature are estimated form theoretical calculation and experiment in each type.
  - Probably, both phases reveal superconductivity at almost same temperature.

Superconductivity in Y_2C_3

-Collaborators-

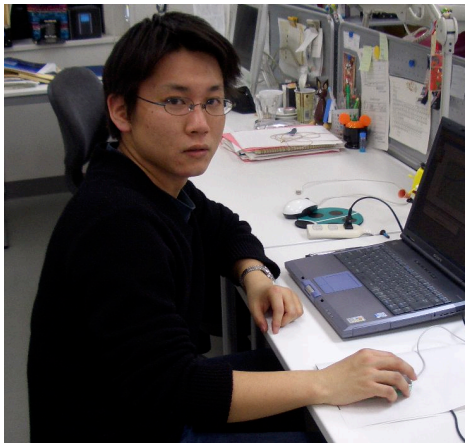

- S. Akutagawa and H. Kitano
- Rietveld analysis
  - K. Osaka, K. Kato and M. Takata (SPring-8)
- Microwave measurement
  - T. Ohashi and A. Maeda (Univ. of Tokyo)
- NMR
  - A. Harada, Y. Miyamichi, H. Mukuda, Y. Kitaoka (Osaka Univ.)

Susceptibility & Resistivity of Y_2C_3

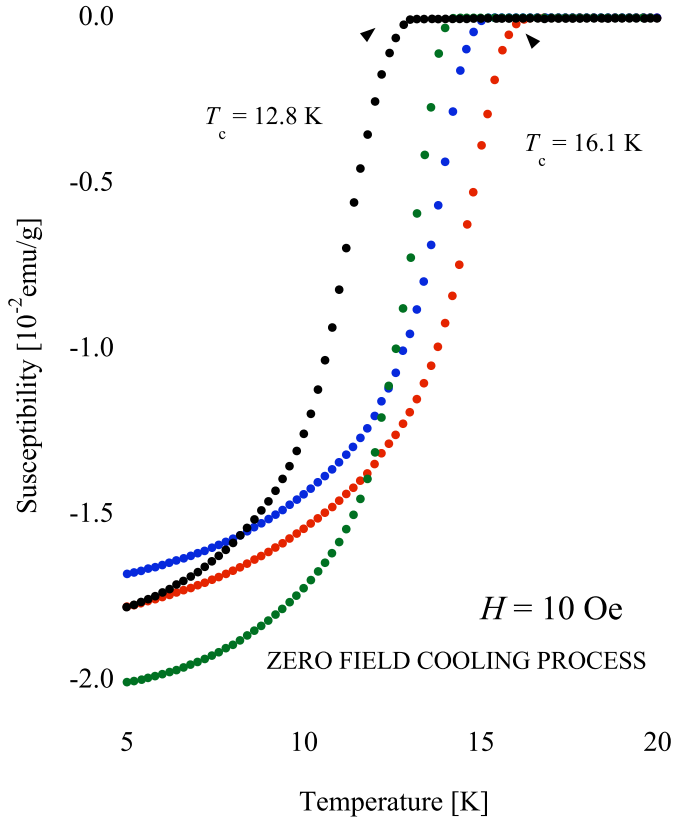

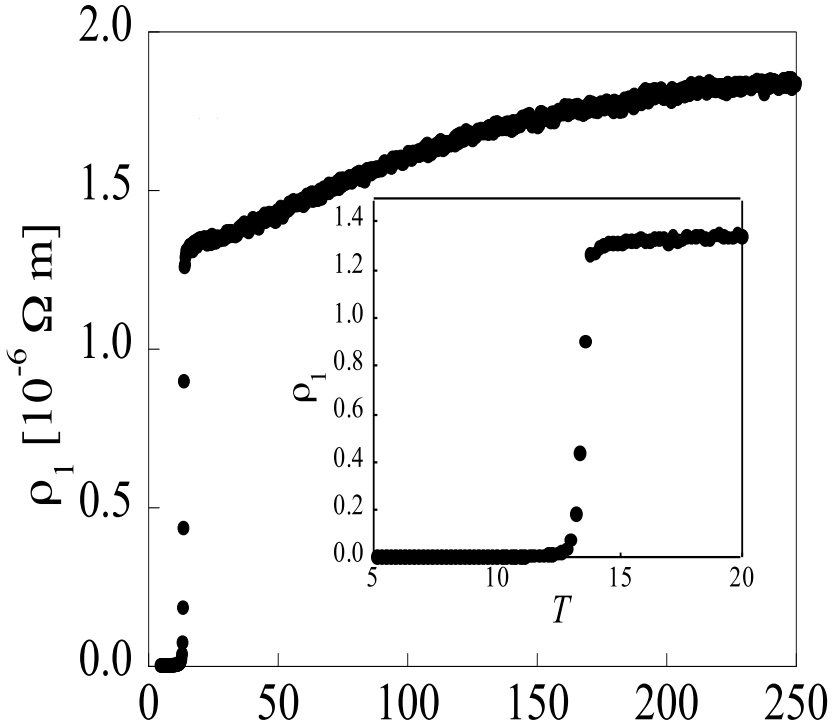

We successfully synthesized high quality Y_2C_3 samples.

T_c is controllable by synthesis condition.

Aoyama-Gakuin University

Rietveld analysis of Y_2C_3 - high-T_c phase (18 K)

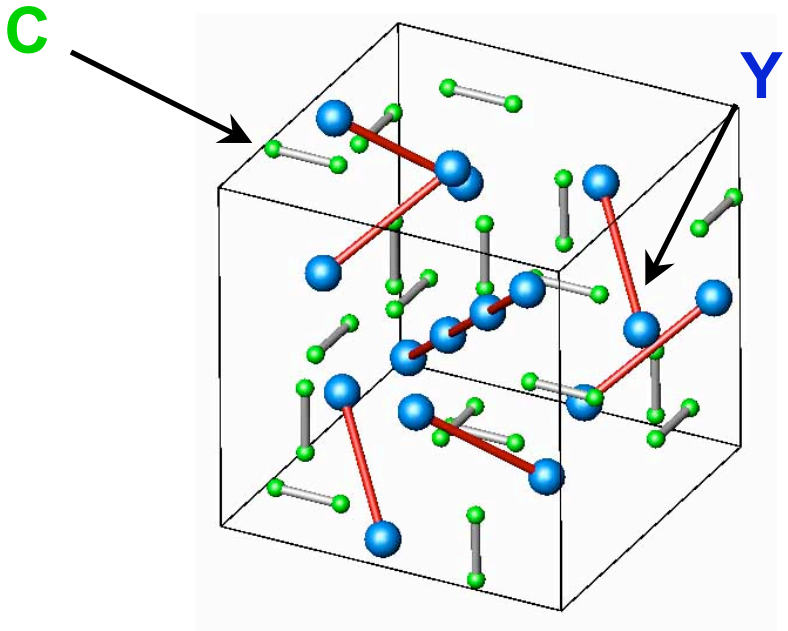

Structure type : Pu_2C_3 type

Space group : $I\bar{4}3d$

Y atoms are aligned along the <111> direction and C atoms form dimers.

Crystallographic parameters

a [Å]		8.187099
Y	x	0.049705
	y	0.049705
	z	0.049705
	g	0.995977
	B	0.441354
C	x	0.294788
	y	0
	z	0.25
	g	0.866852
	B	0.937075

Comparison between low-T_c and high-T_c material in Y_2C_3

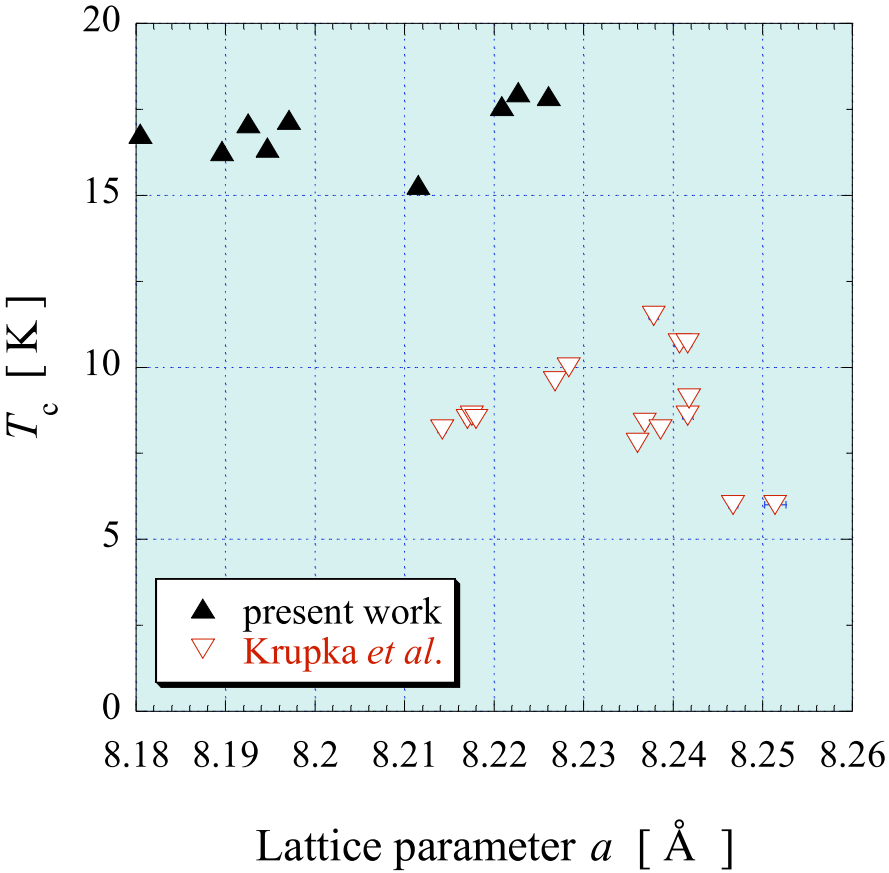

High-T_c material
our work : 8.18~8.23Å

Low-T_c material
Krupka's work : 8.214~8.251Å

The lattice constant, a, of high-T_c material is shorter than that of low-T_c material.

Refined Structure Parameters

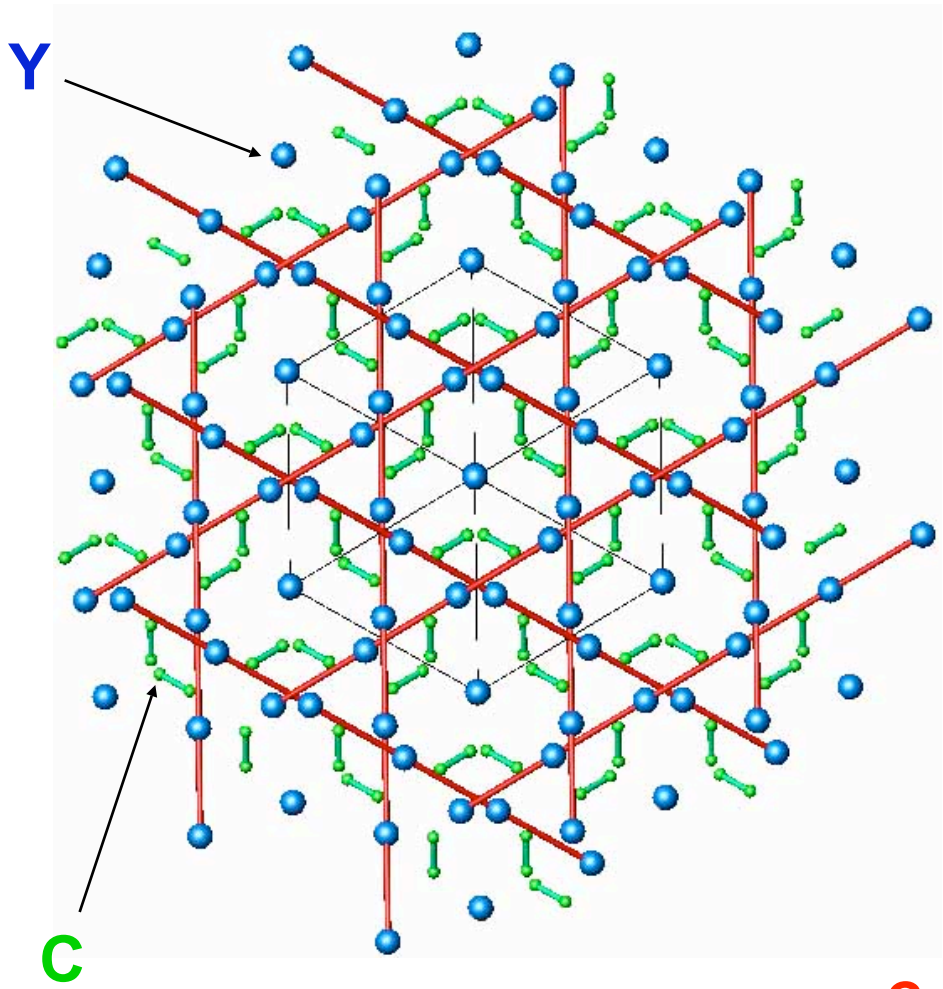

View from [111] direction

High-T_c material

(our work)

$d_{C\text{-}C}$: 1.3134 Å

$d_{Y\text{-}C}$: 2.4876 Å

$d_{Y\text{-}Y}$: 3.5451 Å

Low-T_c material

(V.I. Novokshonov *et al.*)

$d_{C\text{-}C}$: 1.5298 Å

$d_{Y\text{-}C}$: 2.556 Å

$d_{Y\text{-}Y}$: 3.5652 Å

C-C distance of high-T_c material is shorter than that of low-T_c material.

Macroscopic parameters

T_c vs. γ

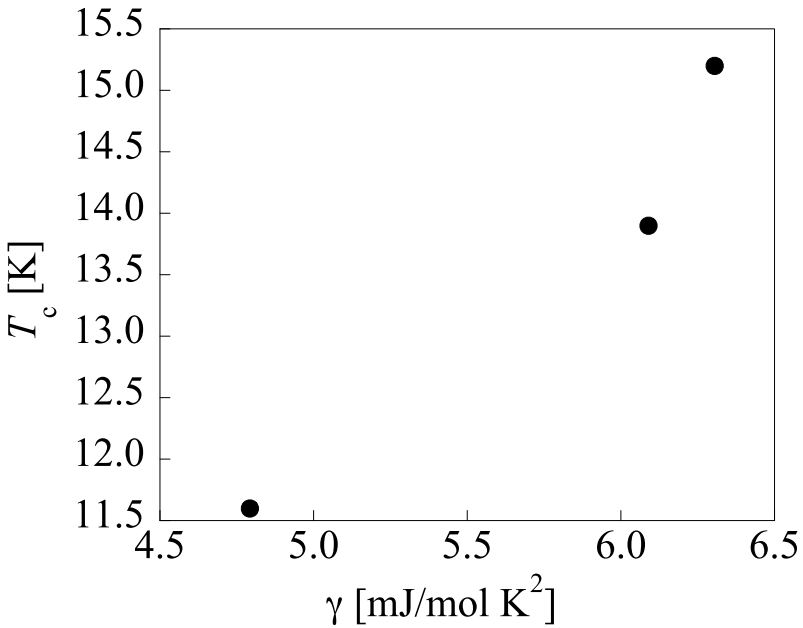

T_c vs. $2\Delta_0/k_B T_c$

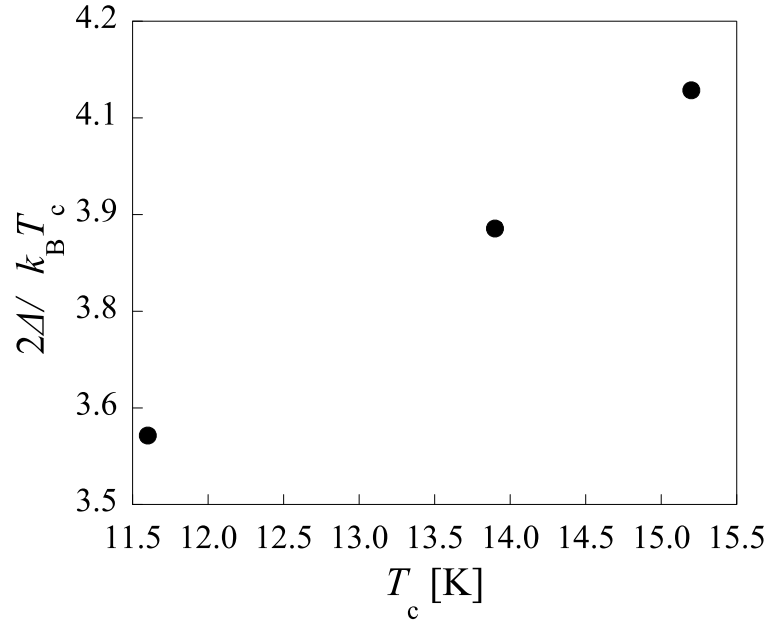

T_c depends on γ.

$2\Delta_0/k_B T_c$ increases with increasing T_c.

Various parameters of Y_2C_3
Comparison with various T_c phases

T_c (K)	11.6	13.9	15.2
γ (mJ/mol·K^2)	4.7	6.0	6.3
θ_D (K)	540	530	530
$\mu_0 H_{c2}(0)$ (T)	22.7	24.7	26.8
$2\Delta/k_B T_c$	3.6	3.9	4.1

Relationship between γ and T_c

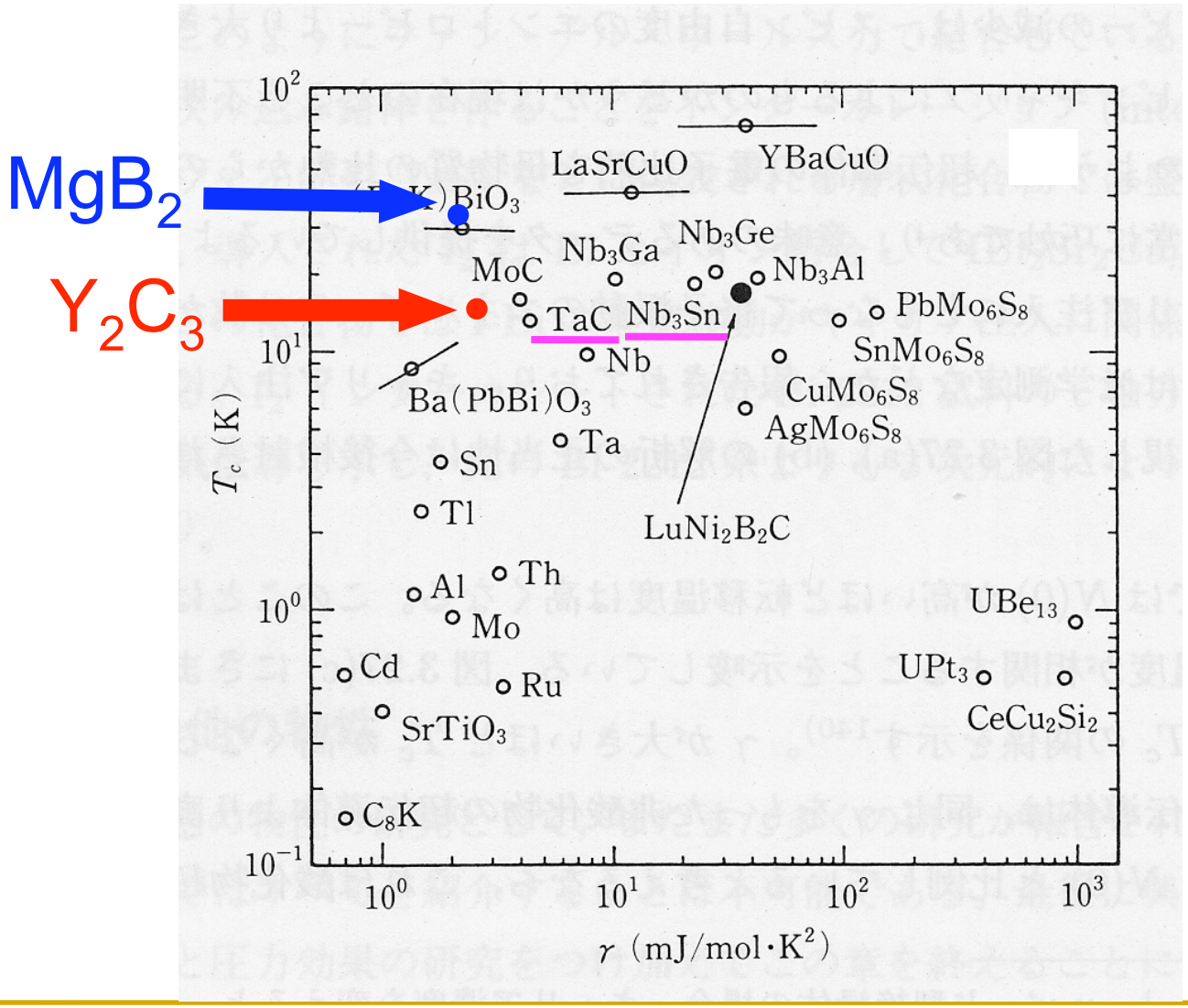

^{13}C NMR Knight shift : singlet or triplet?

Temperature dependence of Knight shift

Knight shift is decreased below T_c.

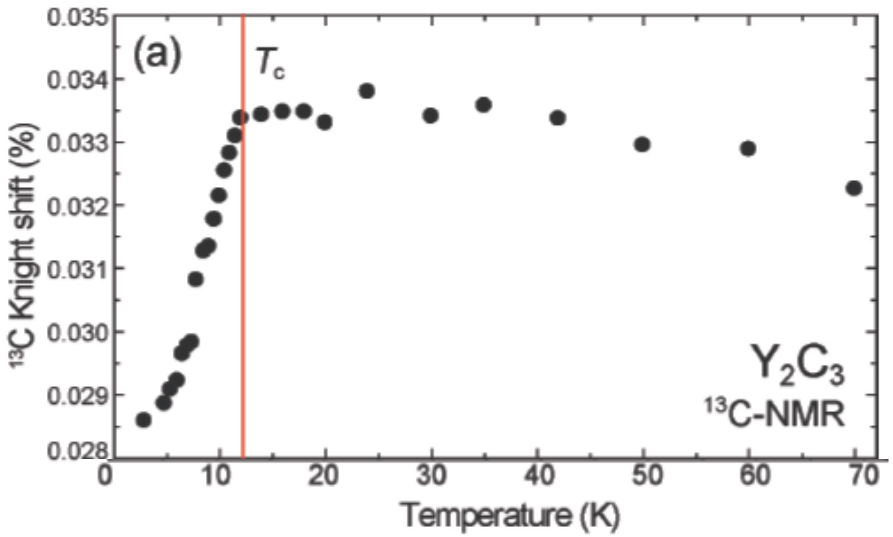

Spin singlet

A. Harada et al., J. Phys. Soc. Jpn. **76(2)** (2007) 023704/1-4.

Aoyama-Gakuin University

^{13}C NMR $1/T_1$: Two-gap superconductor ?

$$T_1T \propto 1/N(E)$$

We observed <u>two</u> components in 1/T dependence.

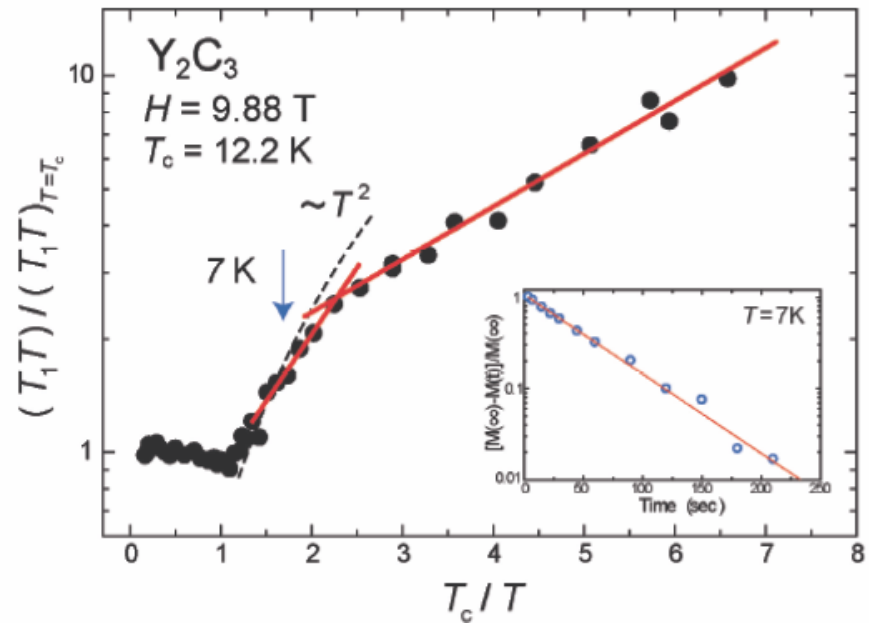

Two isotropic gaps exit in Y_2C_3.

Large gap: $2\Delta_\alpha/K_BT_c = 5$

Small gap: $2\Delta_\beta/K_BT_c = 2$

Dotted line shows ~T^2 (line node).

The inset shows a simple exponential recovery curve of nuclear magnetization

A. Harada et al., J. Phys. Soc. Jpn. **76(2)** (2007) 023704/1-4.

Aoyama-Gakuin University

Superconducting state of La_2C_3 & Y_2C_3 probed by μSR

- S. Kuroiwa, Y. Saura (Aoyama-Gakuin Univ.)
- A. Koda, R. Kadono (KEK)

Sesquicarbide Ln_2C_3 (Ln = La, Y)

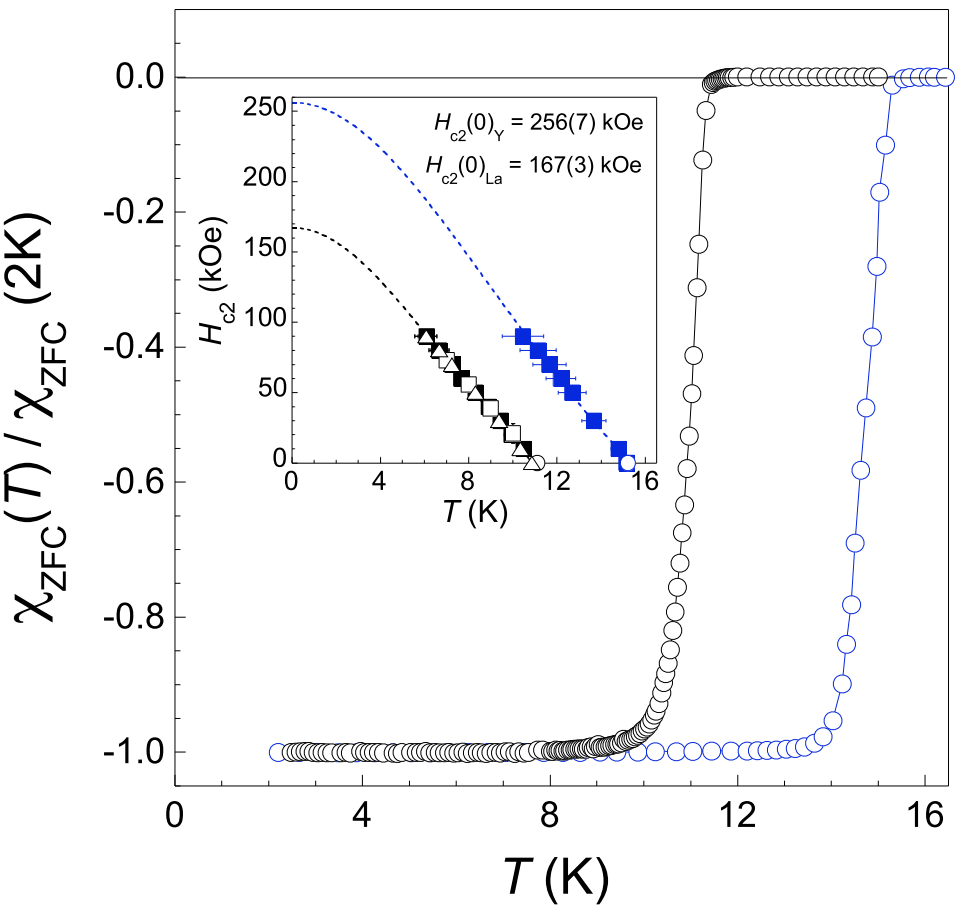

La_2C_3

T_c ~ 11 K

$H_{c2}(0)$ ~ 167(3) kOe

$\xi_{GL}(0)$ ~ 44(1) A

Y_2C_3

T_c ~ 15 K

$H_{c2}(0)$ ~ 256(7) kOe

$\xi_{GL}(0)$ ~ 36(1) A

μSR Results

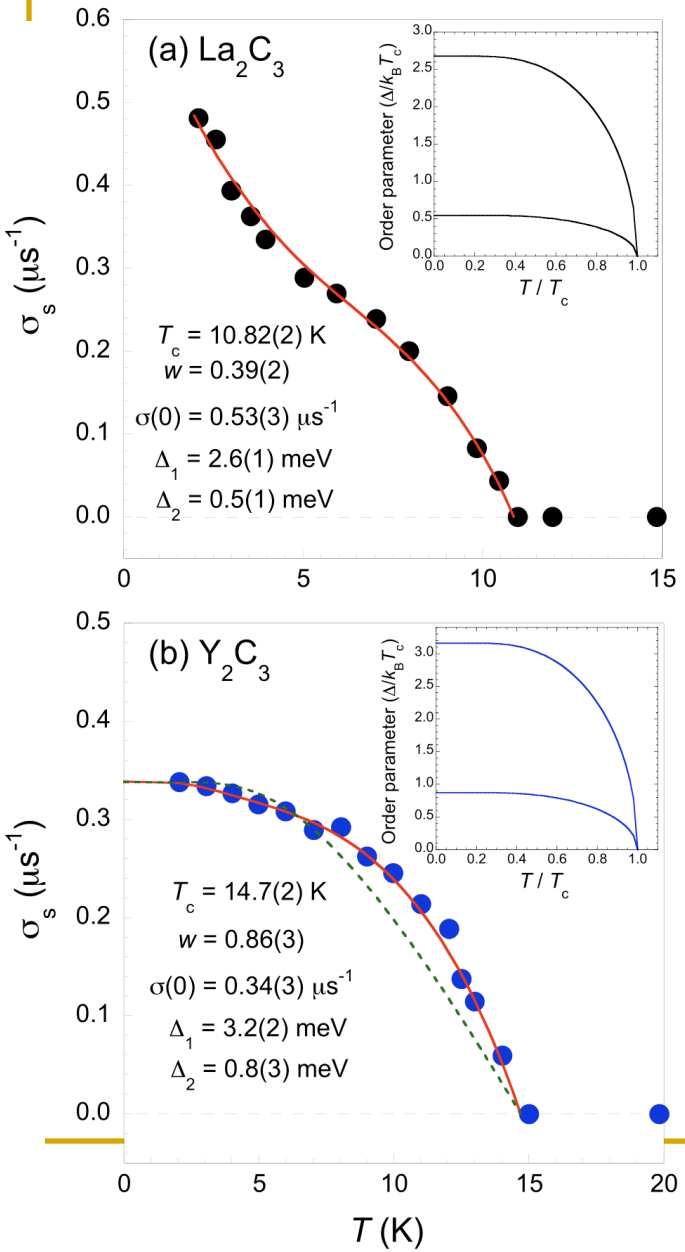

Red curves : Two-gap model

$$\sigma(T) = w\delta\sigma(\Delta_1, T) + (1-w)\delta\sigma(\Delta_2, T)$$

$$\delta\sigma(\Delta, T) = 2\sigma(0)/k_B T \int f(\varepsilon, T)\,[1-f(\varepsilon, T)]d\varepsilon$$

$$f(\varepsilon, T) = (1+\exp(\varepsilon^2+\Delta(T)^2)^{1/2}/k_B T)^{-1}$$

w : ratio between two gaps

$\boldsymbol{k_B}$: Boltzmann constant

$\boldsymbol{f(\varepsilon, T)}$: Fermi distribution function

$\Delta(T)$: BCS gap energy

Green dashed curve : BCS weak coupling

Aoyama-Gakuin University

Parameter	La_2C_3	Y_2C
a (A)	8.795(1)	8.238(1)
$T_{c\text{-onset}}$ (K)	11.1	15.3
$H_{c2}(0)$ (kOe)	167(3)	256(7)
ξ_{GL} (A)	44(1)	36(1)
Two-gap analysis		
H (kOe)	2.5	5.0
$\sigma(0)$ (μs^{-1})	0.53(3)	0.34(3)
$\lambda(0)$ (A)	2990(30)	3730(160)
w	0.39(2)	0.86(3)
$\Delta_1(0)$ (meV)	**2.6(1)**	**3.2(2)**
$\Delta_2(0)$ (meV)	**0.5(1)**	**0.8(3)**
$2\Delta_1/k_BT_c$	**5.4(3)**	**5.0(4)**
	1.0(3)	**1.2(5)**

Summary

- New type-I superconductivity in B-doped SiC.
- Two gap superconductivity in Y_2C_3 (from NMR).

- First observation of phonon dispersion by IXS in CaAlSi.
- H-T phase diagram has been made for single crystalline Ag-clathrate system